IMPLEMENTATION OF Z-SOURCE RESONANT CONVERTER FOR POWER FACTOR CORRECTION AND ELECTRIC VEHICLE APPLICATIONS

A DISSERTATION

SUBMITTED IN PARTIAL FULFILLMENT OF THE REQUIREMENTS FOR THE AWARD OF THE DEGREE

OF

MASTER OF TECHNOLOGY

IN

POWER ELECTRONICS AND SYSTEMS

Submitted by:

AYUSH KUMAR SRIVASTAVA

2K20/PES/08

Under the Supervision of

PROF. NARENDRA KUMAR II

DEPARTMENT OF ELECTRICAL ENGINEERING

DELHI TECHNOLOGICAL UNIVERSITY

(Formerly Delhi College of Engineering)

Bawana Road, Delhi-110042

MAY, 2022

DELHI TECHNOLOGICAL UNIVERSITY

(Formerly Delhi College of Engineering)

Bawana Road, Delhi-110042

CANDIDATE'S DECLARATION

I, **(Ayush Kumar Srivastava), 2K20/PES/08** student of **M.Tech (Power Electronics & Systems)**, hereby declare that the project Dissertation titled **"Implementation of Z-Source Resonant Converter for Power Factor Correction and Electric Vehicle Applications"**, which is submitted by me to the **Department of Electrical Engineering, Delhi Technological University, Delhi** in partial fulfillment of the requirement for the award of the degree of **Master of Technology**, is original & not copied from any source without proper citation. This work has not previously formed the basis for the award of any Degree, Diploma Associateship, Fellowship or other similar title or recognition.

Place: Delhi   **Ayush Kumar Srivastava**

Date: 08/06/22   **2K20/PES/08**

DEPARTMENT OF ELECTRICAL ENGINEERING

DELHI TECHNOLOGICAL UNIVERSITY

(Formerly Delhi College of Engineering)

Bawana Road, Delhi-110042

CERTIFICATE

I hereby certify that the Project Dissertation titled **"Implementation of Z-Source Resonant Converter for Power Factor Correction & Electric Vehicle Applications"** which is submitted by **[Ayush Kumar Srivastava], 2K20/PES/08 [Department of Electrical Engineering], Delhi Technological University, Delhi** in partial fulfillment of the requirement for the award of the degree of **Master of Technology**, is a record of the project work carried out by the student under my supervision. To the best of my Knowledge, this work has not been submitted in part or full for any degree or Diploma to this University or elsewhere.

Place: Delhi   **Prof. Narendra Kumar II**

Date: 08/06/22   **SUPERVISOR**

DEPARTMENT OF ELECTRICAL ENGINEERING

DELHI TECHNOLOGICAL UNIVERSITY

(Formerly Delhi College of Engineering)

Bawana Road, Delhi-110042

<u>ACKNOWLEDGMENT</u>

I wish to express my sincerest gratitude to **Prof. Narendra Kumar II** for his continuous guidance & mentorship that he provided me during the project. He showed me the path to achieve my target by explaining all the tasks to be done & explained to me the importance of this project as well as its industrial relevance. He was always ready to help me and clear my doubt regarding any hurdles in this project. Without his constant support and motivation, this project would not have been successful.

Place: Delhi   **Ayush Kumar Srivastava**

Date: 08/06/22   **2K20/PES/08**

ABSTRACT

The Z-Source Converter is discussed in this study in the context of EV battery charging apparatus. The concept is illustrated using the Z-source resonant converter, which is one of the topology that could be used for charging electric vehicle batteries. The Z-Source Resonant Converter (ZSRC) implements Power Factor Correction (PFC) and controls the voltage at the output side automatically that too simultaneously, thanks to the Z-Source Inverter (ZSI), without going for any control circuitry or extra semiconductor devices, as traditional PFC converters do. To put it another way, the ZSN is a single-stage PFC converter family. Furthermore, because the ZSN is not affected by Shoot-Through States, it is appropriate for high-power applications, thereby increasing system stability and adding a boost function. This project describes and analyses the ZSRC-based Battery Charging System's operational principle.

CONTENTS

LIST OF FIGURES

LIST OF TABLES

LIST OF SYMBOLS

ω	Angular Frequency
ϕ	Phi
η	Eta
Δ	Delta
A	Ampere
V	Volts
μ	micro
θ	Theta
Ω	Ohm
C	Capacitance
L	Inductance
F	Farad
H	Henry
DI_b	Device Current Conduction Index (DI) for a Boost Type Resonant Converter
DI_{ZSN}	Device Current Conduction Index (DI) for a Z-Source Resonant Converter
$P_{sw_b}^{p.u}$	Switching Power Loss for a Boost Type Resonant Converter
$P_{sw_{ZSN}}^{p.u}$	Switching Power Loss for a Z-Source Resonant Converter

LIST OF ABBREVIATIONS

PF   Power Factor

FF   Form Factor

THD   Total Harmonic Distortion

ZSN   Z-Source Network

EVSE   Electric Vehicle Supply Equipment

VS   Voltage Source

CS   Current Source

PFC   Power Factor Correction

CCM   Continuous Conduction Mode

CRM   Critical Conduction Mode

DCM   Discontinuous Conduction Mode

ZSRC   Z-Source Resonant Converter

BRC   Boost Resonant converter

VSI   Voltage Source Inverter

p.u   Per Unit

OBC   On-Board Charger

EV   Electric Vehicle

BCS   Battery Charging System

PWM   Pulse Width Modulation

USB   Universal Serial Bus

PV   Photovoltaic

CHAPTER 1

INTRODUCTION

1.1 GENERAL

Electric vehicles (EVs) have grown in popularity in the automotive industry due to the several benefits they provide, such as better energy security, improved fuel economy, lower fuel prices, and lower pollutants. Electric vehicles (EVs) are powered by one or more electric motors and rechargeable battery packs. Efficiency improvement, environmental sustainability, operation, and decreased reliance on fossil energy resources are all advantages of EVs. However, driving range, recharging time, battery expense, and extra mass and weight are all disadvantages of using an electric car. As the electric vehicle market grows, we must address the issues by encouraging new ideas and advancements. One of the big inconvenience related with EV is conductive battery charging, which is inconvenient and dangerous. The simple notion of wireless power transfer battery charging [1],[2],[3] can be used to overcome this.

1.2 WIRELESS CHARGING SYSTEM

Unlike plug-in electric vehicles, wireless battery charging does not require the use of a power cord. Recent improvements in the field of power electronics in wireless power transmission for EVs are being explored for the alleviation of fuel-powered internal oxidisation engine-driven cars [4, 5, 6]. Because it is a viable alternative, the development of electric vehicles has attracted the interest of both customers and researchers. Between generating stations and consumers, wireless power transmission eradicates present high tension power transmission lines, cables, towers, and substations, enabling for global integration of electrical generation plants. [7].

Nikolas Tesla a well-known developer of wireless power transfer, advocated the transmission of electric power using the air as a medium [7]. Electrical power is transferred through time-dependent magnetic fields, electric fields, or microwaves rather than through cables. Even for charging electric vehicles, Nikolas Tesla, known as the "Father of Wireless," was the first to think about wireless power

transmission and demonstrate the flow of energy over wires, which is dependent on electrical conductivity [8].

For EV battery charging technologies, various approaches have been developed [4, [9], [10], [11]. In terms of power output, efficiency, and distance, many methods have approached the capability. The development of battery charging techniques for electric vehicles, as well as the impact of an electric vehicle, are discussed in this project. Figure 1.1 depicts the fundamental block diagram of a EV Battery Charging System
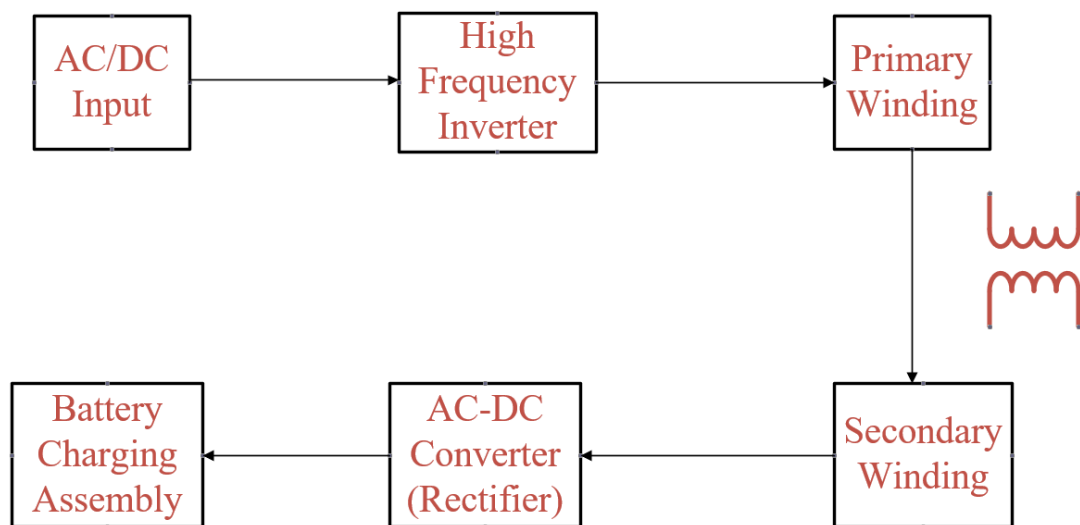
FIGURE 1.1 DATA FLOW DIAGRAM OF BCS METHODOLOGY

1.3 WIRED CHARGING SYSTEM

Battery Chargers normally incorporate some form of voltage regulation to control the charging voltage applied to the battery. The choice of charger circuit technology is usually a price - performance trade off. Some examples are as follows:

i. Switch Mode Regulator:

To control the voltage, it employs pulse width modulation (PWM). Low power dissipation when input and battery voltages vary widely. Linear regulators are more efficient, but they are also more complex.

To smooth the pulsed waveform, a large passive LC (inductor and capacitor) output filter is required. Because the size of the needed transformers, inductors, and capacitors is inversely related to the working frequency, component

size is determined by current handling capability but can be lowered by utilising a higher switching frequency, commonly 50 kHz to 500 kHz. EMI and electrical noise are produced when large currents are switched.

ii. Series Regulator:

Less complex, but more lossy - requires a heat sink to dissipate heat in the series, and a voltage-dropping transistor to absorb the difference between the supply and output voltages. The regulating transistor receives all of the load current, hence it must be a high-power device. It does not require an output filter because there is no switching. As a result, the design is free of radiated and conducted emissions, as well as electrical noise. As a result, it's well suited to low-noise wireless and radio applications. They are also smaller because there are fewer components.

iii. Shunt Regulator:

Shunt regulators are prominent in PV systems due to their low cost and ease of design. A switch or transistor placed in parallel with the solar panel and storage battery controls the charging current. When the voltage reaches a specified level, the PV output is shorted (shunted) through the transistor, preventing the battery from overcharging. By discharging the battery through the shunt if the battery voltage exceeds the PV supply voltage, the shunt also protects the PV panel from harm caused by reverse voltage. Series regulators have greater control and charge characteristics than parallel regulators.

iv. Buck Regulator:

A step down DC-DC converter is built within a switching regulator. They are energy efficient and have minimal heat loss. They can tolerate large output currents and produce less RF interference than traditional switch mode regulators. A straightforward transformerless design with minimal switch stress and a modest output filter.

v. Pulsed Charger:

It makes use of a switchable series transistor. The transistor stays on at low battery voltages and conducts the source current directly to the battery. The series transistor pulses the input current as the battery voltage approaches the target regulating value to keep the voltage stable. It dissipates less heat since it is a switch mode supply for part of the cycle, and the output filters can be smaller because it is a linear supply for part of the cycle. Using modest increments of charge at

increasingly higher charge levels during charging, pulsing allows the battery to stabilise (recover). The polarisation of the cell is reduced during rest times. This method allows for faster charging than a single long-term high-level charge.

vi. USB Charger:

A group of computer and peripheral device manufacturers developed the USB specification to replace a slew of proprietary mechanical and electrical connectivity protocols for transferring data between computers and external devices. It had a two-wire data connection, a ground (earth) line, and a 5 volt power cable from the host device (the computer) to power the external devices. The USB port has been unintentionally used to offer a 5 volt power source not just to power peripheral devices directly, but also to charge any batteries in these external devices. In this instance, the charge control circuitry needed to protect the battery must be built within the peripheral device itself. Data rata was mentioned in the original USB specification.

Power always flows from the host to the device, but data can flow in both directions. For this reason the USB host connector is mechanically different from the USB device connector and thus USB cables have different connectors at each end.

vii. Inductive Charging:

The term "inductive charging" does not apply to the technique of charging a battery. It relates to the charger's design. The input side of the charger, which is connected to the AC mains electricity, is made up of two transformers. The transformer's primary winding is placed in a unit linked to the AC mains supply, while the secondary winding is housed in the same sealed unit that holds the battery and the rest of the conventional charger electronics. This allows the battery to be charged without having to connect to the mains or expose any contacts that could provide an electric shock to the user.

1.4 LITERATURE REVIEW

Proposed by electric utilities and academics, the V2G facility of the Smart Grid envisages the ability of electricity generating utilities to level the demand on their generating capacity by drawing energy from the batteries of EVs connected to the grid during the daylight hours of peak demand and returning it to the vehicles during

periods of low demand during the night. Quite apart from the inconvenience, it would require charging stations to be capable of bi-directional power transfer incorporating inverters with precisely controlled voltage and frequency output to feed the energy back into the grid. It would also require the support of a massive communications network to manage the distributed power flows, the billing and feed-in buy back transactions.

Wireless Power Transfer (WPT) methodology transmit power through an electromagnetic field in the absence of any tangible connection between the transmitter and receiver [119-121]. Latest breakthroughs in view of this sector have spearheaded furthermore demanding structural prerequisites being recommended and studied by researchers, such as improved efficiency [122-126], linkage deviation [127, 128], unfamiliar object recognition [120, 130], and regulation at the output end [131-133]. Electronics engineering is important in these studies and drives WPT technology development.

Wireless power transfer (WPT) for electric vehicle (EV) battery chargers is now being researched for convenience, reliability, and environmental adaptation [62]. The WPT charger technology permits the person who is driving vehicle to position and charge the battery without coming out of the car in a motionless application. EVs could also be charged while driving through the embedded transmit coils along the lines of a Dynamic Wireless Power Transfer charging system [117] (Figure 1.2). A properly-designed storage system for energy and charging has a potential to reduce strength of an electric car battery by 20% [118], resulting into decreased weight and cost.
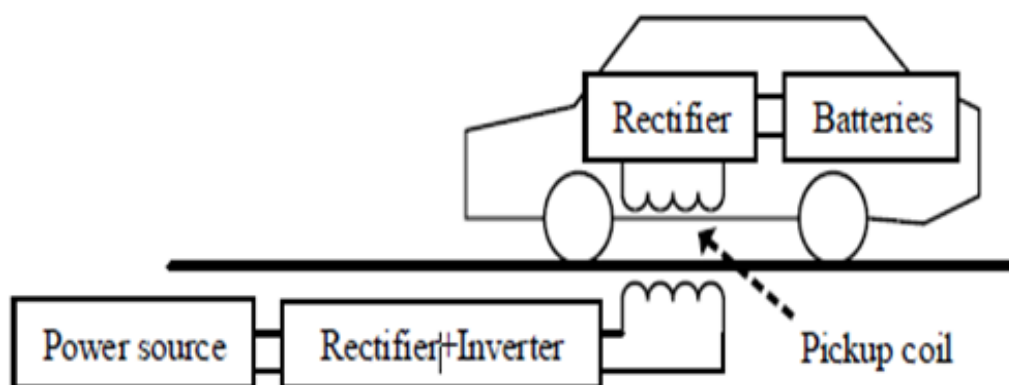
FIGURE 1.2 WPT SYSTEM CONFIGURATION FOR OLPT

CHAPTER 2

POWER FACTOR CORRECTION AND ITS IMPORTANCE

2.1 GENERAL

The power factor is the ratio of the active power utilised by a load (P_{act}) in Kilowatts (KW) to the apparent power supplied to a circuit (P_{apr}) in Kilovolt Amperes (or in KVA). Power Factor is the measure of effective use of electrical energy. The phase of the load current lags or leads the phase of the voltage depending on whether the load is inductive or capacitive, thus causing reactive power (P_{reac}) to grow.

If the current signal has significant malformation when compared to a sinusoidal signal, the power factor will fall much less than 1.0. Harmonic current must be reduced to bring the power factor close to 1.

Below is the power factor triangle that shows the relation between power factor, active and inactive power.
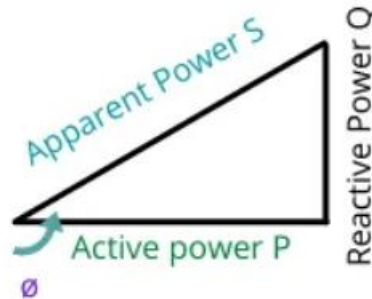
FIGURE 2.1 POWER FACTOR TRIANGLE

Power factor formula:
As shown on the PF triangle above,

$$\text{Power Factor} = \frac{P}{S} \qquad (2.1)$$

Where S is apparent power (KVA); P is active power (KW). The cosine of the phase angle of voltage and current is the power factor, as shown in the power triangle.

$$PF = \cos(\phi) \tag{2.2}$$

Replacing the Value of PF:

$$\frac{P}{VI} = \cos(\phi) \tag{2.3}$$

The capacity of a circuit to accomplish work at a particular moment is defined by real (or active) power. The total amount of power utilised to operate electrical equipment is measured as apparent power..

Power factor is a popular expression of efficiency of energy using. And is expressed as a number less than or equal to 1.

2.2 CAUSES FOR LOW POWER FACTOR

Inductive loads are the main cause of low power factor. Large industrial applications have large inductive loads, these loads consume active power in KW, and also need for proper operation a consumption of reactive power from the power grid (KVAR) to sustain a magnetic field. The higher the reactive power the lower the power factor.

The AC input is rectified, and a bulk capacitor is connected directly after the diode rectifier bridge in various electronic power supplies. This sort of serviceability interconnection uses a lot of peak input current, creates a great amount of harmonics, and has a poor input power factor (PF) and total harmonic distortion (THD).

2.3 NECESSITY OF PFC

Manufacturers of practically every single equipment that uses substantial power from a mains outlet, along with experts in the large-electrical sector, are apprehensive about power factor. Not only are engineering concepts at issue, but also regulations requiring compliance with power-factor standards.

2.3.1 Importance Of Power Factor And Power Factor Correction

i. Legal Framework:

The earliest attempt to legislate for ac mains power interference was in 1899, to prevent incandescent lamps from flickering. However, one of the most significant laws was passed in 1978, when IEC 555-2 stipulated that power factor correction measures need to be included in the design of consumer electronics.

In countries like U.S their energy department guidelines have made it mandatory for the use of measuring devices to have a PFof 0.9 at full capacity of rated output in the power supply, which implies that designs with internal power supplies demand Active Power Factor Correction (PFC).

Throughout Atlantic, the European Union has enacted the EN 61000-3-2 electronic equipment standard, which limits the 39th order harmonic for devices with input current carrying capacity of magnitude less than or equal to 16 Ampere (A) per phase.

A slew of countries are following Europe's lead and enacting more rigorous rules. Governments in numerous countries like China, Japan, and Australia have amended several provisions in EN 61000-3-2 guidelines for harmonics in power-supply field.

ii. Supply consequences:

Producers and distribution firms should be prepared to offer the maximum voltage of waveform and current magnitudes at every moment. A power factor (PF) of lower than 1.0 results in increased costs, which impacts the users severely as they need to pay a higher price for low power-factor loads. As a result, ensuring highest power factor is a "win-win" situation for everyone.

iii. Coherence and Harmonic Distortion Issues:

This not only shifts the effective current peak away from the voltage waveform in time, but it also introduces switching waveforms with a lot of harmonic content, which may exacerbate the current waveform's distortion. The widespread deployment of PCs and other IT devices roughly coincided with the emergence of this type of supply. These developments paved the way for the current legislative climate.

2.4 APPROACHES FOR PFC

Active (switching) PFC, partial-switching PFC, and passive (static) PFC are the three types of PFC techniques.

```
                          ┌─────────────────────┐
                          │  SINGLE PHASE PFC   │
                          └─────────────────────┘
         ┌───────────────────────┼───────────────────────┐
┌──────────────┐   ┌──────────────────────┐   ┌──────────────┐
│ PASSIVE PFC  │   │ PARTIAL SWITCHING PFC│   │  ACTIVE PFC  │
└──────────────┘   └──────────────────────┘   └──────────────┘
                        ┌──────────────────────┴──────────────┐
                ┌─────────────────┐              ┌──────────────────┐
                │ LOW FREQUENCY   │              │ HIGH FREQUENCY   │
                └─────────────────┘              └──────────────────┘
                              ┌──────────────────┴──────────────┐
                        ┌─────────────┐                   ┌──────────┐
                        │ RESONANT    │                   │  PWM     │
                        └─────────────┘                   └──────────┘
                                    ┌──────────────────────┴──────────────┐
                            ┌────────────────┐                    ┌──────────────┐
                            │ NON ISOLATED   │                    │  ISOLATED    │
                            └────────────────┘                    └──────────────┘
                            ┌────────────────────┐              ┌───────────────────┐
                            │ BUCK BOOST PWM     │              │ FLYBACK PWM       │
                            │ RECTIFIER          │              │ RECTIFIER         │
                            └────────────────────┘              └───────────────────┘
```
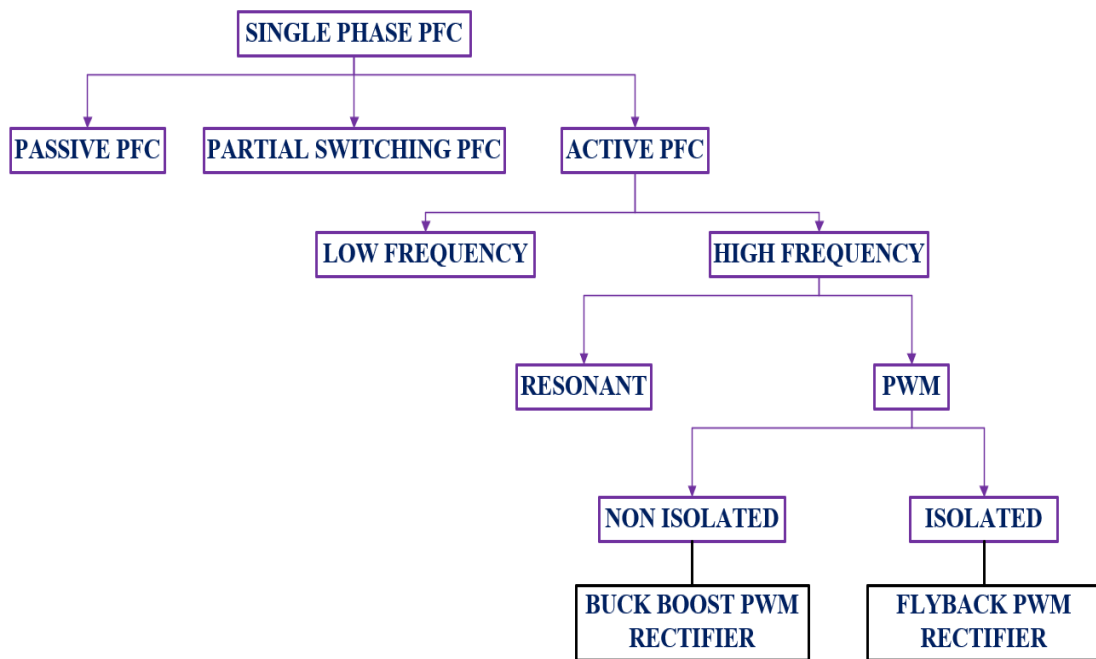
FIGURE 2.2 FLOW CHART DEPICTING VARIOUS PFC TECHNIQUES

A switching PFC circuit's basic topology is the boost chopper. Numerous circuit configurations, such as parallel switching device PFC, interleaved PFC, and bridgeless PFC, are utilised depending on the power supply capacity. There are also three different modes of current conduction:

i. Continuous Conduction Mode abbreviated as CCM sends constant current signal to a switching reactor.

ii. Critical conduction Mode abbreviated as CRM enables switching devices at zero current interval.

iii. Discontinuous Conduction Mode abbreviated as DCM transmits current at a set interval.

Different control approaches are needed for various conduction modes.

2.4.1 Passive Power Factor Correction Approach

A voltage doubler rectifier is shown in Figure 2.3 as an example of a passive PFC circuit. The input current waveform for this circuit is shown in Figure 2.4. The reactor (L) aids in power factor improvement, while diodes and smoothing capacitors convert AC to DC. A big reactor and capacitors are required because the passive Power Factor

Correction (PFC) electrical circuit operates at a supply frequency interval of 50 or 60 Hz. As a result, passive PFC is commonly employed in power supply with limited capacity.
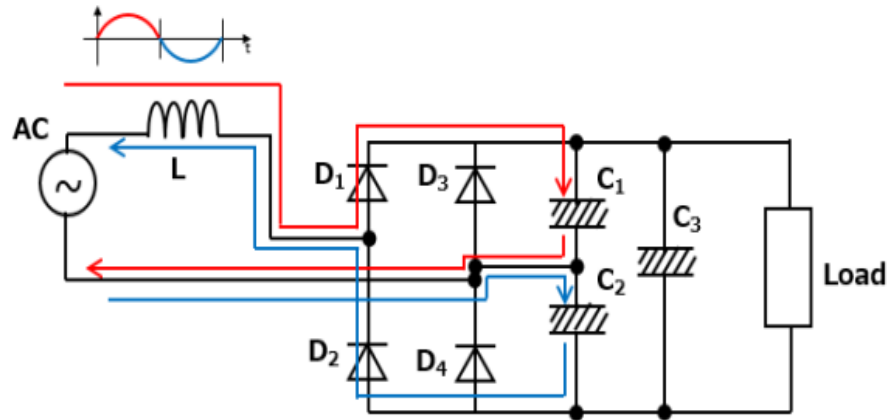
FIGURE 2.3 CIRCUIT DIAGRAM OF PASSIVE POWER FACTOR CORRECTION (PFC) ELECTRICAL CIRCUIT
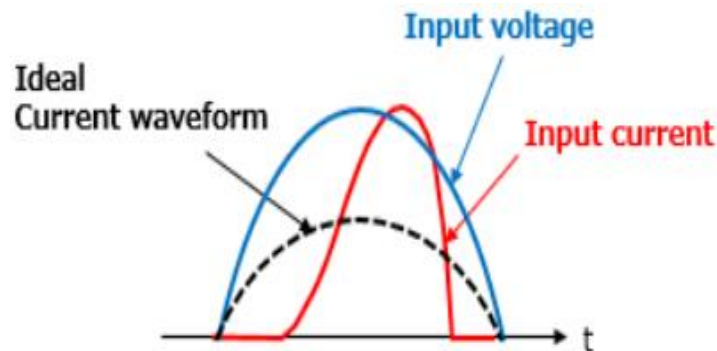
FIGURE 2.4 WAVEFORM OF INPUT CURRENT FOR PASSIVE POWER FACTOR CORRECTION (PFC)

2.4.2 Patial-Switching Power Factor Correction Approach

A switching device is used in this PFC circuit, which switches a few times every half cycle. When zero current is flowing in the case of passive Power Factor Correction (PFC), this Power Factor Correction (PFC) approach partially activates the switching element and passes current to the reactor. This PFC improves the power factor by increasing the period over which the input current flows. In view of the fact that energy can be stored in the reactor, a partial-switching PFC circuit can boost the output voltage

higher than the supply voltage. Furthermore, since it executes switching functions occasionally in each half of supply cycle, a partial-switching Power Factor Correction (PFC) circuit can be designed to have pretty low switching losses. A partial-switching PFC circuit is shown schematically in Figure 2.5. An input current waveform for this circuit is shown in Figure 2.6.
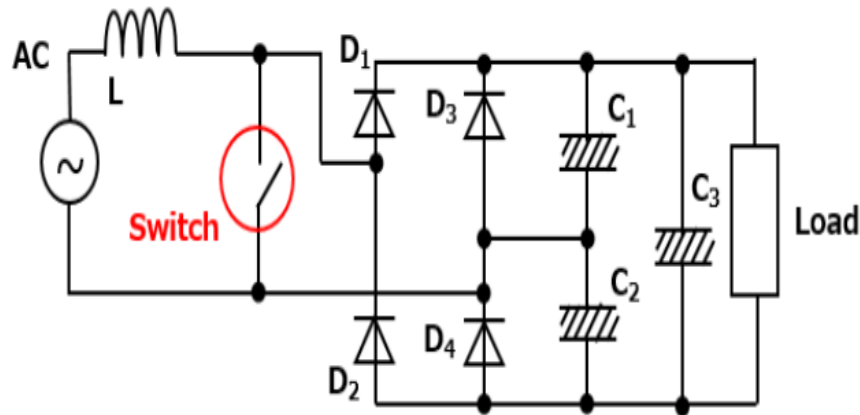
FIGURE 2.5 PARTIAL-SWITCHING POWER FACTOR CORRECTION (PFC) CIRCUIT
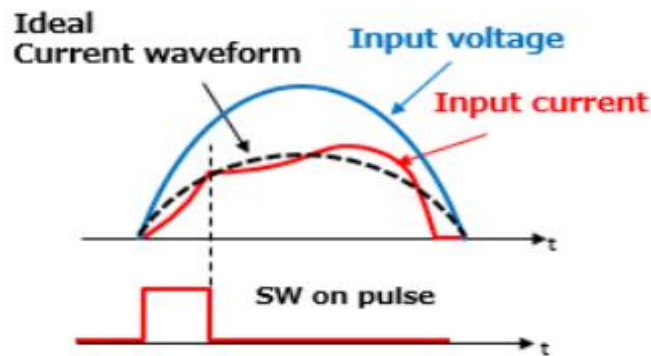
FIGURE 2.6 CURRENT WAVEFORM OF A PARTIAL-SWITCHING POWER FACTOR CORRECTION (PFC) CIRCUIT

2.4.3 Active-Switching Power Factor Correction Approach

This section discusses the boost converter (boost chopper) depicted in Figure 2.7, which is often used for active Power Factor Correction (PFC). CCM, CRM, and DCM are the three types of active Power Factor Correction (PFC) circuits based on the current conduction mode utilised. The active PFC circuit regulates current by switching on and off MOSFETs, synchronises the voltage and phase of power-line, and closes the gap between the input current waveform and a sine wave. The current

MOSFET turn-on path is highlighted by arrow #1 in Figure 2.8, whereas the MOSFET turn-off path is highlighted by arrow #2. A example current waveform of a MOSFET Q1 and output diode D5 of a CCM Power Factor Correction (PFC) circuit is shown in Figure 2.6.
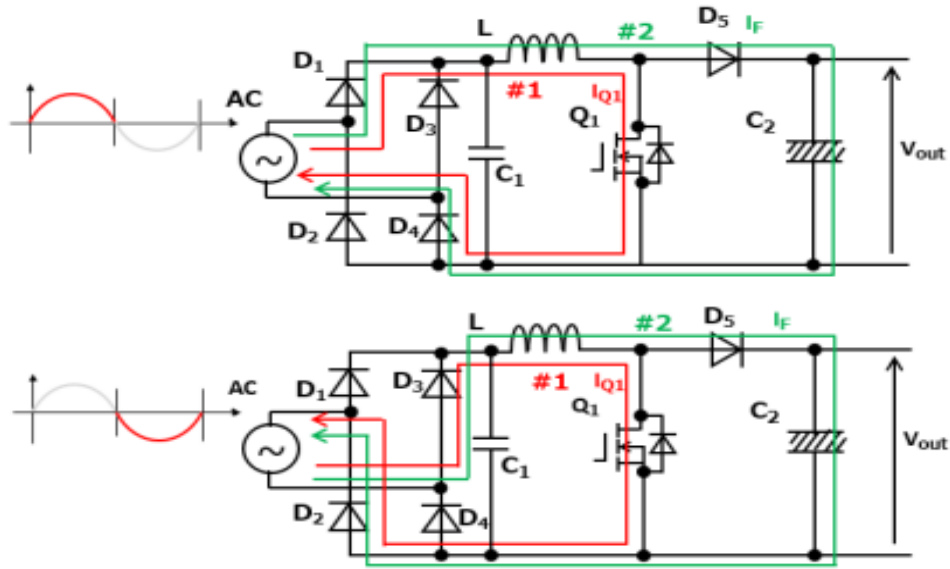
FIGURE 2.7 BASIC ACTIVE POWER FACTOR CORRECTION (PFC) CIRCUIT AND ITS CURRENT PATHS
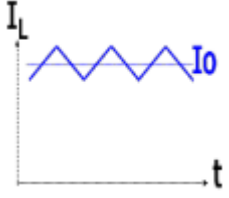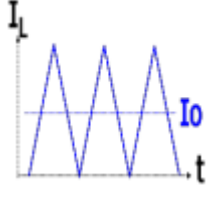
FIGURE 2.8 TYPICAL WAVEFORMS IN CONTINUOUS CONDUCTION MODE (CCM) MODE
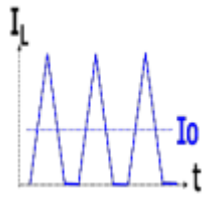
2.4.3.1 Process blueprint of various active power factor correction modes

According to the current conduction modes, Active Power Factor Correction (PFC) circuits are categorised into three categories. They are distinct in their features. Critical

conduction mode and Discontinuous Conduction Mode are typically utilised for low-capacity commercial power supplies, while Continuous Conduction Mode is used for power supplies with a relatively big capacity. Their properties are outlined in Table 2.1.

TABLE 2.1 OVERALL PATTERN OF THREE DIFFERENT CURRENT CONDUCTION MODES

Conduction Mode	Control Method	Output Capacity and Applications	Advantages and Disadvantages	Reactor Current Waveform
CCM	PWM (Pulse Width Modulation) control	Used In industrial energy sources, used for power demand larger than 300 W	• Input current has minor ripples. • Peak current is small. • If the PFC diode has a long reverse recovery time, it reduces overall circuit efficiency and produces noise problems (t_{rr})	
CRM	PFM (Pulse Frequency Modulation) control	Used in LCD TVs, PCs, and commercial power supplies for	• The reactor current has minor ripples. • Peak current is high.	

		power consumption of 75 to 300 W.	• Low switching loss and zero current switching.	
DCM	PWM control, PFM & Valley Switching control	Used as LED lighting power supplies, small-capacity power supplies, and for power usage between 25 and 100 W.	• The reactor current has huge swirls. • Low switching loss and zero current switching. • Peak current is high. • During zero-current times, shows valley oscillation.	

2.5 BENEFITS OF POWER FACTOR CORRECTION (PFC)

Following are different upsides of going for Power Factor (PF) Improvement Topologies in a Circuit:

i. Power bill savings:

   Power factor correction (PFC) avoids reactive energy penalisation, reduces KVA demand, and decreases power losses in the installation's transformers and conductors.

ii. Increased power supplying capacity:

   The power available at the secondary of an MV/LV transformer is increased by installing PFC technology on the low voltage side. A high power factor boosts an electrical system's efficiency by allowing components to work more efficiently.

iii. Smaller installation:

For the same active power, the adjusted arrangement consumes less current., due to which the conductor cross-section can be lowered when Power Factor Correction (PFC) technology is installed.

iv. Minimised Voltage dips:

Installing capacitors reduces voltage dips upstream of the PFC device, preventing network overload and lowering harmonics..

CHAPTER 3

ONBOARD CHARGER

3.1 GENERAL

OBCs transform AC electricity into a DC voltage that is used to charge the vehicle's battery pack from an external power supplying source. Other roles performed by OBCs include charge rate monitoring and protection. The table below shows the industry charging norms for OBC systems (Table 2). Some Level 1 systems and AC Level 2 OBCs require isolation. OBCs are bypassed when using DC Fast Chargers, which plug straight into the quick charging port.

TABLE 3.1 ORGANISATION OF EVSE LEVELS 1, 2 AND 3

Charging Standards			
EVSE Type	Level 1 (Residential)	Level 2 (Commercial)	Level 3 (Fast Chargers)
Voltage	120/230V AC	208/240 V AC	300-600 V DC
Current	12-16 A	15-80 A	400 A
Phase	Single	Single/Split	Poly
Power Supply	1.44-1.92 KW	3.1-19.2 KW	120-240 KW
Charging Time	17 Hours	8 Hours	30 Minutes

On-board chargers (OBCs) take AC input signal, rectify it to high voltage DC signal, and provide PFC. The resulting DC Voltage signal is sliced into a switched square waveform, which is then used to drive a transformer to generate the appropriate DC voltage. To chop the input signal, isolated gate drivers such the Si8239x, Si823x, Si823Hx, and Si827x are employed.

Using sync FETs under the command of extra cloistered gate drivers, the output voltage is filtered to the final DC voltage. Isolated analogue sensors, such as the Si892x, can be used to monitor the output voltage in order to provide closed cycle feedback to the system controller.

A secluded CAN bus can be used to monitor and control the entire system. To seclude the CAN, Si86xx and Si88xx digital isolators and digital isolators with integrated DC/DC power converters are employed.

3.2 FUNDAMENTAL SETUP OF A STANDARD ON-BOARD CHARGER

As shown in Figure 3.1, a typical battery charger of On-Board Type (OBC) has a structure with two level containing PFC unit on front side and a high frequency transformer with a DC-DC Converter. The two-stage architecture has a high overall cost and complexity, despite the fact that each stage can be optimized separately.
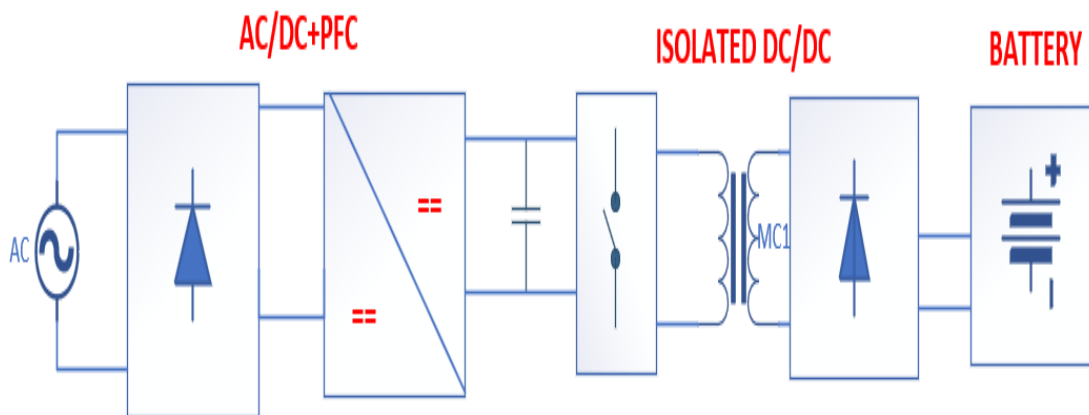
FIGURE 3.1 FUNCTION BLOCK DIAGRAM OF A TYPICAL ON-BOARD CHARGER

OLPT applications have also been investigated using single-stage OBC converters. They simultaneously regulate the system output voltage while correcting the power factor (PF). In single phase single stage (S^2PFC) topologies, previous research has been done [35, 39]. Most of them simply have one switch, resulting in minimal overall costs and ease of use. Owing to the fact that these converters descend from the flyback, they all place a great deal of strain on the transistor or semiconductor devices, necessitating the employment of a superior voltage handling capacity with a lot of transposition disadvantages. Consequently, the S^2PFC technique is suitable where reduced-power is utilized (i.e., shorter than 100W) where affordability is a primary consideration [40].

The forward-unit PFC converter is combined with a resonant converter in other topologies. A boost converter incorporated with a half-bridge LLC converter is used as an example of this architecture in [41. This topology's power specification is restricted.

Many different topologies have been investigated [21, 43, 59], however the Z-Source converter will be chosen as a benchmark in this work.

CHAPTER 4

BATTERY CHARGER FOR ON-BOARD USE

4.1 GENERAL

There are various kinds of topologies that are used for PFC correction at the front end stage like Cuk, Sepic, Interleaved Sepic, Flyback etc. but the most conventional used topology is boost converter based.

4.2 CONVENTIONAL BOOST BASED ON-BOARD BATTERY CHARGER (OBC)

In current EV battery chargers, the standard boost converter [21] is the most widely utilised PFC converter for the front end stage. Figure 4.1 depicts a boost-converter-based OBC using a Series Resonant Converter (SRC) as the DC/DC stage, which is the most common converter for Battery Charging Applications.[60].
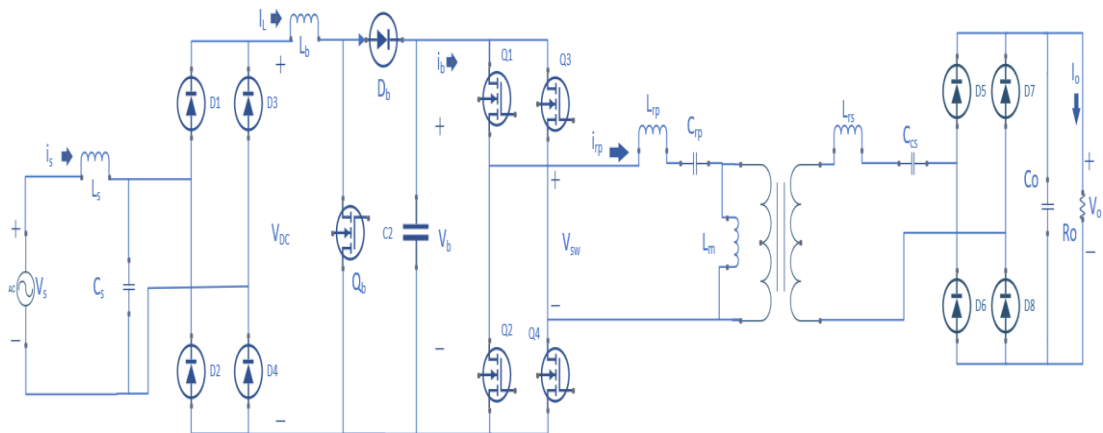
FIGURE 4.1 BOOST-CONVERTER-BASED OBC

The traditional boost based PFC converter has a greater power efficiency, good power factor (PF) at input end, superior power density, and budget friendly [43]. Despite this, the ripple current of the boost capacitor (C_b) is relatively high [21, 43]. Just as its power delivering capacity rises, the system input rectifier losses impair the efficiency dramatically and heat dissipation measures become necessary. The boost based PFC

converter is hence suitable for small to moderate power usage requirements upto 3.5 kW. Designers usually parallel individual semiconductors or use expensive diode semiconductor modules for power levels exceeding that, which raises the overall system price [21, 43]. Furthermore, the boost converter switch is operated under severe switching conditions, resulting in large switching losses and limiting the system's switching frequency range. Finally, the reverse recovery of a boost diode (D_b) generates a lot of electromagnetic interference (EMI), which can cause unanticipated shoot-through states that harm the system or trigger protection and cause an unexpected system shut down [55, 59, 61]. A new PFC converter is used in this project to address some of these issues.

4.3 PROPOSED ZSRC BASED ON-BOARD BATTERY CHARGER (OBC)

This study proposes the Z-source based Resonant converter as a revolutionary PFC Conversion Topology. The ZSI fundamental topology was created in [62] and is mostly used for governing voltage at the output end. For On Board Charging requirements, the Z-Source Inverter can be positioned in the Power Factor Correction level, followed by a secluded DC/DC converter, i.e a typical Series Resonant Converter. The Z-source resonant converter is the OBC-designed architecture (ZSRC). Figure 4.2 illustrates the circuit schematic. [60] first instituted the core of this kind of technology in 2010, but only for DC/DC type conversion.

Inherent PFC is a unique proposition dealt by ZSN present in ZSRC, without going for additional devices which is not available in typical PFC converters. It does so by preventing shoot-through states in the H-bridge inverter topology and introducing a control variable (shoot-through duty cycle parameter (D_{st})) that could be used as a prototype for shaping the current at input end as a typical sine wave i.e in coherence with the voltage at the input end. This variable enhances the system as well, which is why it's frequently used for voltage regulation [62]. The devised ZSN-based OBC, on the other hand, controls the output voltage with the active state duty cycle parameter (D_{act}), a typical parameter for controlling in Series Resonant Converters. The Z-Source Inverter Topology has exceptional upsides in comparison with various PFC Converter Topologies like boost converter based BCS. We'll go through these in the next section.
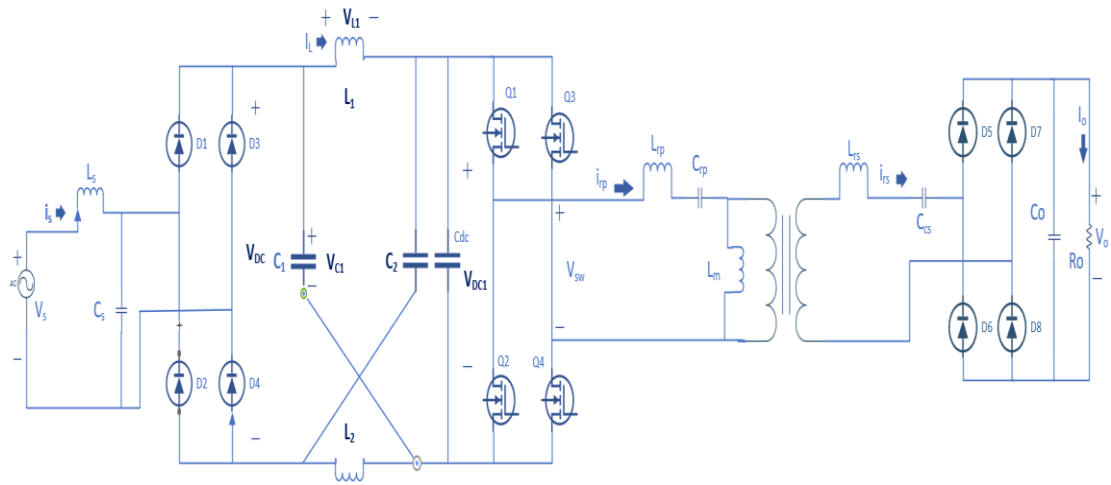
FIGURE 4.2 Z-SOURCE BASED RESONANT CONVERTER

CHAPTER 5

COMPARATIVE ANALYSIS OF BOOST & Z-SOURCE BASED RESONANT CONVERTERS

5.1 GENERAL

Since, VSI provides high-frequency AC power for Wired Mode Of Transmission, VSI is an integral component of a BCS system. Traditional VSI inverters' output voltage is never exceeding than the voltage at the input side, which confines its implementation in low-voltage type or broad-input type situations. Front-end converter topologies, like boost or buck-boost, Z-Source configurations are employed to augment the dc-rail voltage between a DC source and a VSI to overcome this barrier [62, 117].

5.2 COMPARATIVE REVIEW OF WIDESPREAD BRC & NOVEL ZSRC

Following Table 5.1 shows the necessary comparsion between two type of resonant converters. Both, the converters are compared on a standard set of parameters such as component count, failure & degradation rate, heat sink requirement, adeptness etc.

TABLE 5.1 COMPARISON OF BOOST TYPE & Z-SOURCE TYPE RESONANT CONVERTERS

COMPARED PARAMETER	RESONANT CONVERTERS EMPLOYING BOOST CONFIGURATION	RESONANT CONVERTERS EMPLOYING Z-SOURCE CONFIGURATION
COMPONENT COUNT	This type of resonant converter has more number of power semiconductor devices as it uses two capacitors and two semiconductor devices.	This type of resonant converter has two capacitors and no semiconductor devices.

FAILURE & DEGRADATION RATE	As Capacitors and semiconductor devices have the highest failure and degradation rates of any component in a power electronic system (30 % and 21 % , respectively) Consequently, this type of resonant converter has a higher rate of failure & degradation.	As it uses lesser number of components so it possess lesser rate of failure & degradation.
HEAT SINK REQUIREMENT	According to [48], this type of resonant converter uses more number of components, hence a heat radiator is required for the power semiconductors devices and supplementary governing integrated circuits for the switch[63].	As such, there is no requirement of heat sink for this type of resonant converter.
SIZE AND WEIGHT	This type of resonant converter has a larger size & more bulkier, since it uses more number of components with an added heat sink.	Due to the fact that this type of resonant converter uses lesser number of components. Furthermore, it does not require an excess heat sink as well, it has a smaller size & less bulkier.
ADEPTNESS	Boost based resonant converter lacks the	Z-Source based resonant converter could manage

	proficiency to handle unexpected situations like shoot-through condition where due to either by purpose or by EMI noise where both the upper and lower devices of each phase leg are gated on simultaneously.	shoot-through conditions. As a result, random EMI shoot-through will have no effect on system functioning.
COST-EFFECTIVENESS	Owing to the fact that Boost based converter uses more number of components & requires extra heat sink for radiation, the costs involved are high.	Since, this type of resonant converter uses lesser number of components, also it does not require additional heat sink. It is a more budget friendly option.
DURABILITY	Since, this type of resonant converter has a higher rate of failure & degradation due to which it has a shorter lifespan.	As, this type of resonant converter has a lower failure and degradation rate than a standard boost PFC converter. Therfore, it has a longer lifetime.
LOSSES	Owing to the fact that Boost based converter uses more number of components & also a lot of heat is generated when current flows through them. Hence, it has greater value of switching, conduction & thermal losses.	Since, this type of resonant converter uses lesser number of components. Therefore, it possess lower value of switching, conduction & thermal losses with respect to a Boost based resonant converter. • $DI_{ZSN} = [4B]_{p.u}$ • $P_{sw_{ZSN}}^{p.u} = [4B]_{p.u}$

	• $DI_b = [3B + 2]_{p.u}$ • $P_{sw_b}^{p.u} = [B + 4]_{p.u}$	
EFFICIENCY	As this type of resonant converter has more switching, thermal & conduction losses. Therefore, it possess a lower value of efficiency.	This type of resonant converter possess a greater value of eficiency due to lower number of such losses.

CHAPTER 6

MODELLING OF EV BATTERY CHARGING SYSTEM

6.1 GENERAL

The notion of operation, simulation, and observational evidence along with formula evaluation of the different constituent parts used in a Z-Source Inverter (ZSI) based Battery Charging System are described in the subsequent segments.To validate the analysis, simulations of the proposed system were run at (192 W).

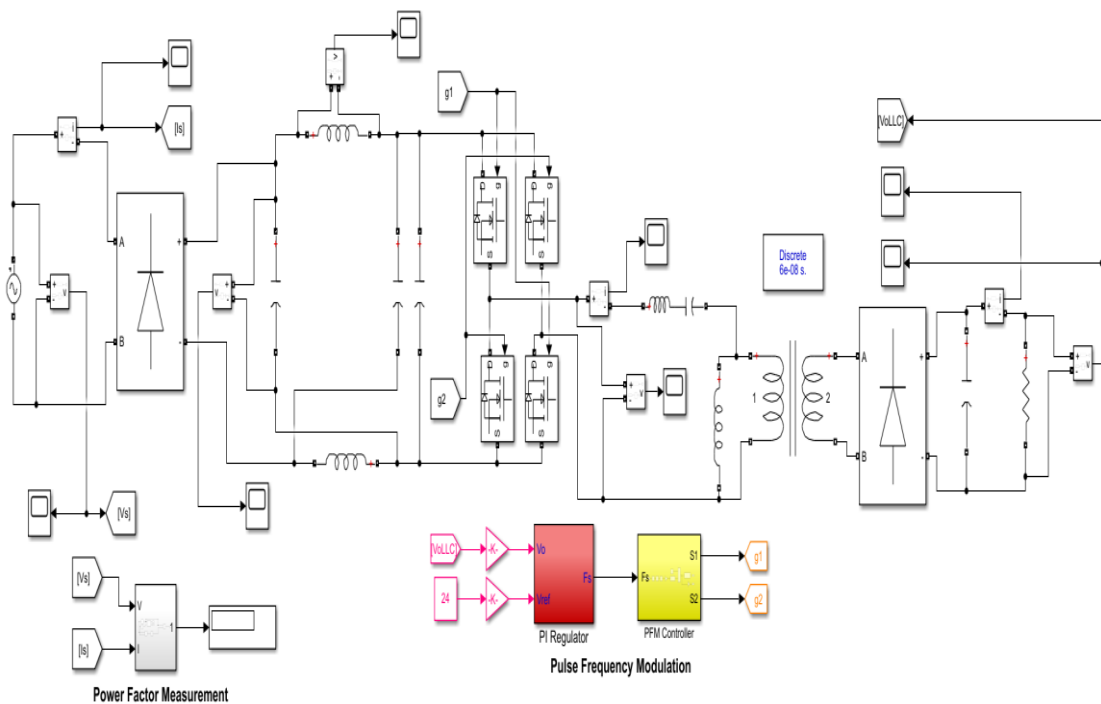

FIGURE 6.1 SIMULINK MODEL OF A Z-SOURCE BASED BATTERY CHARGING SYSTEM

6.2 RECTIFIERS

Rectifiers are broadly divided into two types which are as follows:

i. Half Wave Type Rectifier
ii. Full Wave Type Rectifier

A full-wave rectifier is a circuit that transforms both half cycles of alternating current (AC) to direct current (DC). A half-wave rectifier uses only one-half cycle of the incoming alternating current, as we learned in our tutorial on half-wave rectifiers. Consequently, a full-wave type rectifier is significantly more efficacious than a half-wave type rectifier. Full-wave type rectification is the conversion of both the half cycles of an AC source to DC.

There are two techniques to make a full-wave rectifier. A centre tapped transformer together with two diodes are used in the first way. The Center Tapped Full-Wave Type Rectifier is the designation given to this configuration.

The second variant exercises a conventional transformer along with four bridge diodes. This configuration is known as a Full Wave Bridge Type Rectifier.

As a result, there are two configurations of full wave rectifiers:

i. Full Wave Bridge Rectifier
ii. Centre-tapped Full Wave Rectifier

6.2.1 Full Bridge Diode Type Rectifier

Figure 6.1 illustrates a single-phase full-bridge diode rectifier with R-Load. D1, D2, D3, and D4 are the four diodes that make up this circuit. These are some basic observations about the bridge rectifier in Figure 6.1:

i. D1 and D2 conduct simultaneously, as do D3 and D4. D1 and D3 cannot be on concurrently, according to Kirchhoff's voltage rule around the loop including the source, D1, and D3. D2 and D4 can't both be active at the same time. The load current can be either positive or negative, but not both.

ii. When D1 and D2 are both switched on, the voltage across the load is +Vs. When D3 and D4 are both switched on, the voltage across the load is -Vs.

iii. The peak value of the source is the greatest voltage across a reversed-biased diode. Kirchhoff's voltage law around the source, D1, and D3 loops demonstrates this. The voltage across D3 is -Vs when D1 is switched on.

iv. i_{D1} - i_{D4}, which is symmetric around zero, is the current entering the bridge from the source. As a result, the source current is zero on average.

v. The rms source and load currents are identical. For one-half of the source period, the source current equals the load current, and for the other half, it equals the load

current. The rms currents are equal because the squares of the load and source currents are equal.

vi. Because two periods of output occur for every period of input, the fundamental frequency of the output voltage is 2ω , where ω is the frequency of the ac input. A dc term and the even harmonics of the source frequency make up the Fourier series of the output.
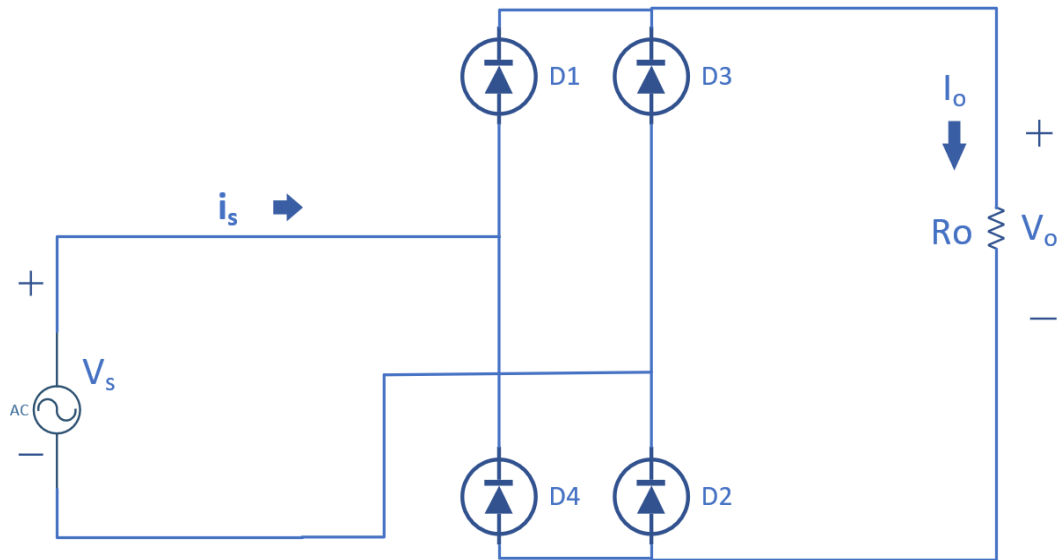
FIGURE 6.2 BLOCK DIAGRAM OF FULL BRIDGE DIODE RECTIFIER
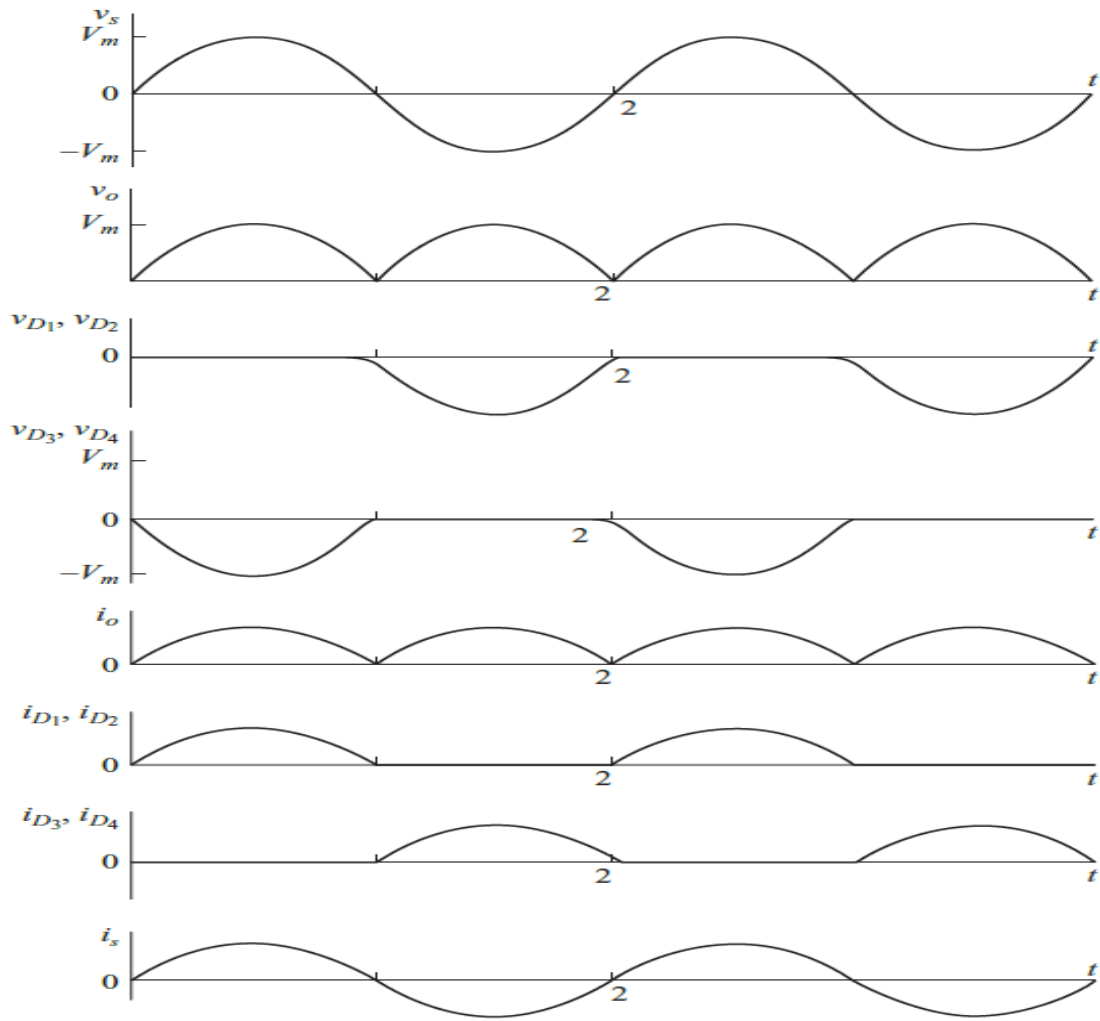
FIGURE 6.3 WAVEFORMS OF VOLTAGES AND CURRENTS IN FULL BRIDGE DIODE
RECTIFIER

Average Output Voltage is given by:

$$V_o = \frac{2V_m}{\pi}$$ (6.1)

$$I_o = \frac{2V_m}{\pi R}$$ (6.2)

Rectifier output voltage is crimped, which means it is made up of both AC and DC components.. These AC components are obnoxious, as they diminish productiveness. As a result, content filters are utilised to reduce ripples, leaving the DC component to

show at the output. Capacitor, inductor, and combination of capacitor and inductor are all significant filters. In most industrial applications, a single phase full bridge diode type rectifier with capacitive filter is employed at the input side because it is a budget friendly and immensely dependable option for low-power-consumption requirements[65].

6.2.1.1 Single phase full bridge diode type rectifier with capacitive filter

Ripples are produced by a rectifier without a filter, resulting in low efficiency and power factor. To reduce output ripples, some energy is held in a capacitor and released during pulses. The single-phase full-bridge diode rectifier with capacitve filter is shown in Figure 6.3. A huge capacitor is immediately across the load terminals, as seen in Figure 6.3. This capacitor receives the pulsing voltage from the rectifier without a filter (see Figure 6.2). The voltage signal across the capacitor rises at the same rate as the half sinewave voltage signal from the rectifier, indicating that the RC charging period is very small. The capacitor voltage does not drop to zero when the rectifier voltage decreases to zero. Instead, during the time that the rectifier is not delivering electricity, the energy stored in the capacitor is discharged through the load. After the capacitor is discharged, the rectifier will not allow current to flow until the rectifier's output voltage surpasses the voltage across the capacitor.
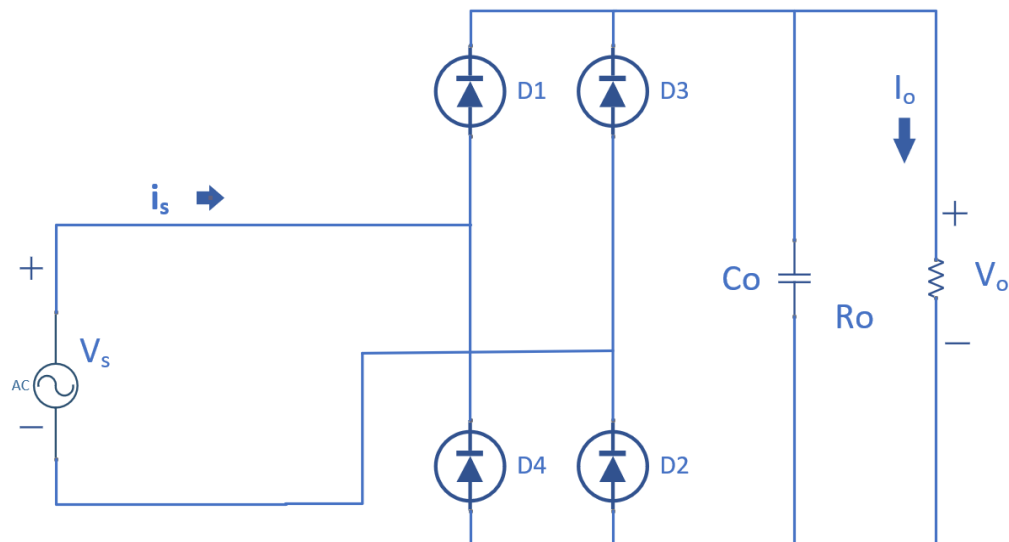
FIGURE 6.4 BLOCK DIAGRAM OF FULL BRIDGE DIODE RECTIFIER WITH CAPACITIVE FILTER

6.2.1.1.1 Full wave bridge rectifier formulae with capacitive filter:

i.   Ripple Voltage Calculation:

Let us assume, during the conduction phase, the charge received by the capacitor equals the charge misplaced by the capacitor.

Ripple voltage from top to top is given by:

$$V_{rpp} = \frac{V_p}{2fRC} \qquad (6.3)$$

Ripple Voltage Maximum Value:

$$V_{rp} = \frac{V_{rpp}}{2} = \frac{V_p}{4fRC} \qquad (6.4)$$

RMS Value of Ripple Voltage:

$$V_{rms} = \frac{V_{rp}}{\sqrt{2}} = \frac{V_p}{\sqrt{2} \cdot 4 \cdot f \cdot R \cdot C} \qquad (6.5)$$

ii.   Average Output Voltage is given by:

$$V_o = V_p - V_{rpp} = V_p\left[1 - \frac{T}{4RC}\right] \qquad (6.6)$$

iii. Average Output Current is given by:

$$I_{dc} = \frac{I_o}{R} \qquad (6.7)$$

iv.   Full Wave Rectifier Ripple Factor (γ):

The undesirable AC component that remains after converting an AC voltage waveform to a DC waveform is known as 'ripple.'

The formula for ripple factor is:

$$\gamma = \frac{V_{rms}}{V_o} = \frac{1}{\sqrt{2}(4fRC-1)} \tag{6.8}$$

Where V_{rms} is the AC component's RMS value, and V_{dc} is the rectifier's DC component.
Note: We want to maintain the ripple factor as low as feasible while building a suitable
rectifier. To eliminate ripples in the circuit, capacitors or inductors might be used.

V. Power factor is given by:

$$PF = \frac{V_{rms}I_{s1}}{V_{rms}I_s}\cos(\phi) \tag{6.9}$$

$$PF = K_d \cdot K_\theta \tag{6.10}$$

The following equation gives the distortion factor K_d:

$$K_d = \frac{I_{s1}}{I_s} \tag{6.11}$$

The following equation gives the displacement factor K_θ:

$$K_\theta = \cos(\phi) \tag{6.12}$$

The displacement factor (K_θ) can be achieved to equal one with a capacitor or inductor,
but the distortion factor (K_d) is increasingly complex to achieve.
Hence, Power Factor (PF) = K_d

vi. The total harmonic distortion factor (THD) is calculated as follows:

$$THD(\%) = 100 \times \sqrt{\frac{1}{K_d^2-1}} \tag{6.13}$$

During the maximum value of the AC input voltage, the capacitor will be charged,
resulting in a large value of maximum input current. The utility is used to feed this

rectifier with extremely distorted current. Regulations will curb the level of current distortion permitted into the supply mains based on harmonic criteria established by the United States and European countries. This holds for all capacitive-filtered rectified AC sinusoidal signals. Every single-phase rectifier takes a pulse of current twice every cycle in order to recharge its capacitor to the source voltage's peak value. The capacitor drains to assist the load between voltage peaks, and the rectifier draws no current from the supply mains. As a result of this behaviour by single-phase rectifier , distorted currents are drawn from the input line when harmonic currents are generated. Low-order current harmonics, on the other hand, are quite large, approaching the fundamental value. The waveform shows a lower fundamental frequency component as well as current harmonics at the 3rd, 5th, 7th, 9th, and higher frequencies. Single-phase bridge type rectifiers used to connect power electronic appliances to supply mains systems may violate international regulations for individual current harmonics and THD (Total Harmonic Distortion) due to their high harmonic content[66].

vii. Full Wave Bridge Rectifier Efficiency (η):

$$\eta = \frac{P_{dc}}{P_{ac}} \tag{6.14}$$

viii. Form Factor of a Full Wave Rectifier (FF):

$$FF = \frac{V_{rms}}{V_o} \tag{6.15}$$

6.2.2 Centre-Tapped Full Wave Type Rectifier

Figure 6.5 depicts the voltage waveforms for the centertapped transformer type rectifier with a resistive load. The following are some fundamental observations about this circuit:

i. Only one diode can conduct at any given moment, according to Kirchhoff's voltage law. The current flowing through the load can be positive or negative, but never negative.

ii. When D1 conducts, the output voltage is +Vs1 and +Vs2 respectively. The secondary voltages of transformers are proportional to the source voltage in the following way:

$$V_{s1} = V_{s2} = V_s \left(\frac{N_2}{2N_1} \right)$$

(6.16)

iii. The upmost voltage across a reverse-biased diode is double the highest value of the load voltage, in accordance with the voltage law proposed by Kirchhoff around the transformer secondary windings, D1, and D2.

iv. The average source current sets to zero since current in both half of the transformer secondary is reflected to the primary,.

v. Between the source and the load, the transformer creates electrical isolation.

vi. Because two cycles of output occur for every input cycle, the fundamental frequency of the voltage at output side is 2ω.

The bridge rectifier's lower peak diode voltage makes it more suitable for high-voltage applications. In addition to electrical isolation, the center-tapped transformer rectifier has only one diode voltage drop between the source and the load, making it ideal for low-voltage, high-current applications.
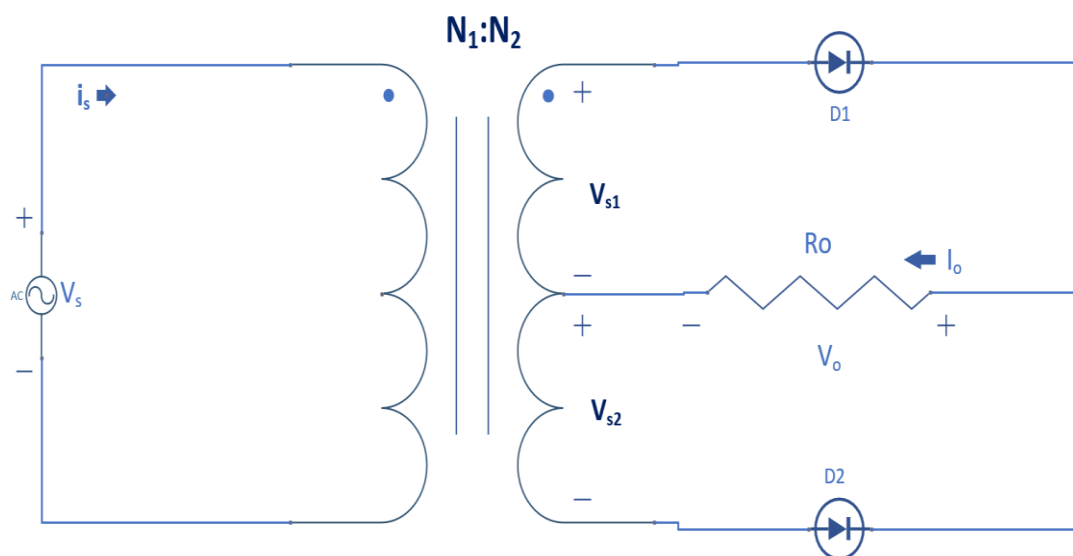
FIGURE 6.5 BLOCK DIAGRAM OF FULL-WAVE CENTER-TAPPED RECTIFIER
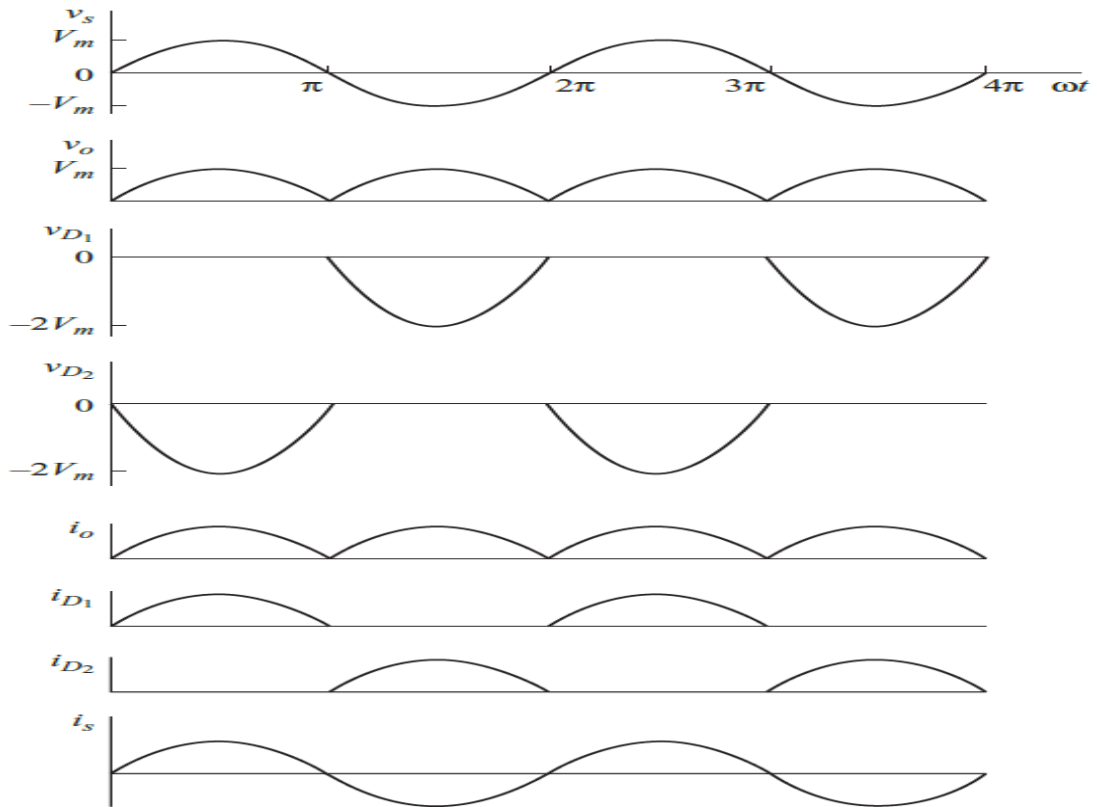
FIGURE 6.6 WAVEFORMS OF VOLTAGES AND CURRENTS IN FULL-WAVE CENTER-
TAPPED RECTIFIER

6.2.2.1 Centre-tapped full wave type rectifier with capacitive filter

As a result of the centre tapped full wave rectifier, we receive a pulsating DC voltage with multiple ripples. This pulsating signal cannot be used for practical purposes.

As a result, we employ a filter circuit, as shown in Figure 6.6, to convert the fluctuating DC signal to stable DC voltage. Here we place a capacitor across the load.
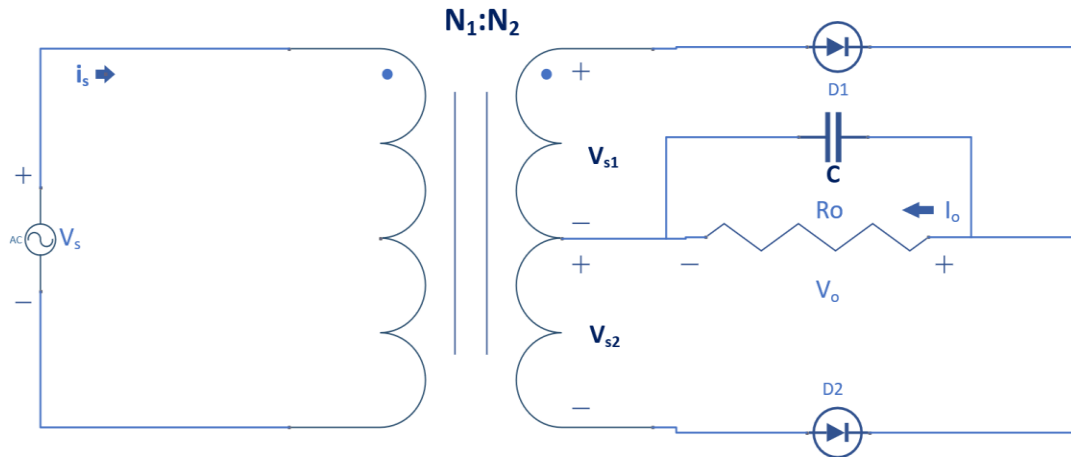
FIGURE 6.7 BLOCK DIAGRAM OF CENTRE-TAPPED FULL WAVE RECTIFIER WITH
CAPACITIVE FILTER

The capacitive type filter circuit's function is to trim ripples and hamper the DC component, enabling it to traverse via different path and over the load. The diode D1 starts to conduct during the positive half-wave. There is no charge on the capacitor.

When an input AC voltage exceeds the capacitor voltage, the capacitor is charged to the maximum value of the input voltage instantaneously. The capacitor voltage equals the supply voltage at this point..

When the applied magnitude of AC voltage dips below that of the capacitor, the capacitor begins to drain at a slow rate, but this is more slowly as compared with the charging of the capacitor, so it does not have enough time to drain completely, and charging recommences.

As a result, around half of the capacitor's charge is discharged. The diode D2 begins to conduct during the negative cycle, and the process begins all over again. Subsequently, the current will flow in the same direction across the load.
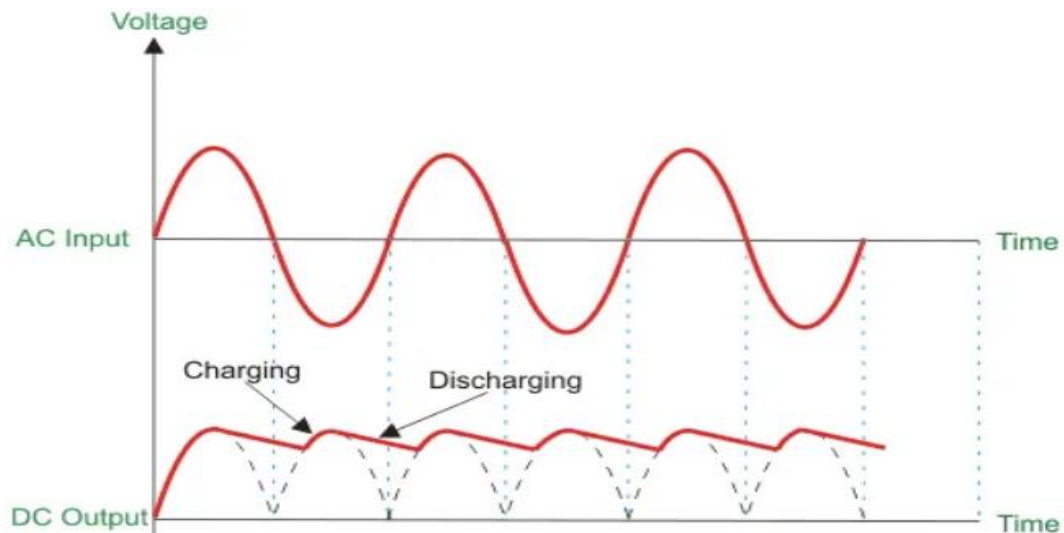
FIGURE 6.8 WAVEFORM OF AC INPUT & DC VOLTAGE IN CENTRE-TAPPED FULL WAVE
RECTIFIER WITH CAPACITIVE FILTER

6.2.2.1.1 Centre-tapped full wave rectifier formulae with capacitive filter:

i. Center-tapped Full Wave Rectifier Efficiency (η):

$$\eta = \frac{P_{dc}}{P_{ac}}$$ (6.17)

$\eta_{max} = 81.2\%$

ii. Centre-tapped full wave rectifier's Form Factor (F.F):

$$FF = \frac{V_{rms}}{V_o}$$ (6.18)

F.F = 1.11

6.2.3 Merits & Demerits Of Full Wave Rectifiers:

The merits of full wave rectifiers are as follows:

i. A full-wave bridge rectifier's efficiency is doubled. Because only half of the input
    signal is used by a half-wave rectifier, this is the case. The efficiency of a bridge
    rectifier is doubled because it uses both parts.

ii. In the output of a bridge rectifier, residual ac ripples (before filtering) are quite low. In a half-wave rectifier, the same ripple % is extremely high. To acquire a constant dc voltage from the bridge rectifier, all you need is a simple filter.

iii. We know that full-wave rectifiers have double the efficiency of half-wave rectifiers. This translates to higher output voltage, TUF, and power.

The demerits of full wave rectifiers are as follows:

i. Full wave rectifiers are more expensive

ii. Full wave rectifiers take up more space than half-wave rectifiers.

6.2.4 Bridge Rectifier Advantages And Disadvantages Over Center-Tap Rectifier

A bridge rectifier has the following advantages over a centre tap rectifier:

i. A bridge rectifier can have a transformer or not. Any regular step-down/step-up transformer will suffice if a transformer is required. In a centre tap rectifier, this luxury is not available. The centre tap transformer, which cannot be replaced, is required for the rectifier's design.

ii. For high-voltage applications, the bridge rectifier is ideal. When compared to a centre tap rectifier, the bridge rectifier has a higher peak inverse voltage (PIV).

A bridge rectifier has the following disadvantage over a centre tap rectifier:

i. A bridge rectifier has four diodes in its construction, which is a substantial disadvantage when compared to a centre tap. On a half cycle of input, two diodes in a bridge rectifier conduct concurrently. Only one diode conducts on a half-cycle in a centre tap rectifier. In a bridge rectifier, this results in a higher net voltage drop between the diodes (it is double the value of the centre tap).

6.2.5 Full-Wave Bridge Rectifier Applications

The full-wave rectifier is used in the design of constant dc voltage power supplies, particularly in general power supplies. A bridge rectifier with an effective filter is appropriate for general power supply applications such as charging a battery, powering a dc device (such as a motor or LED), and so on. A standard power source, however, may not be enough for an audio application. The residual ripple factor in a bridge rectifier is the reason behind this. Filtering ripples has many drawbacks. Specially

designed power supply (based on IC regulators) may be excellent for audio applications.

6.3 Z-SOURCE INVERTER

The ZSI can be used in applications that require voltage boost. The first presentation of the ZSI occurred in 2002 [69]. It's an impedance source converter, not a voltage or current source converter. The impedance network's key feature is that it uses inductors, capacitors, and switches/diodes to boost or buck the voltage in the circuit. It's a single-stage power conversion system that combines a dcdc boost converter with an inverter. The structure of the Z-source converter is depicted in Figure 6.8. It consists of a two-port network that comprises of inductors L_1 and L_2 and capacitors C_1 and C_2 coupled which are employed in an X shape fashion.
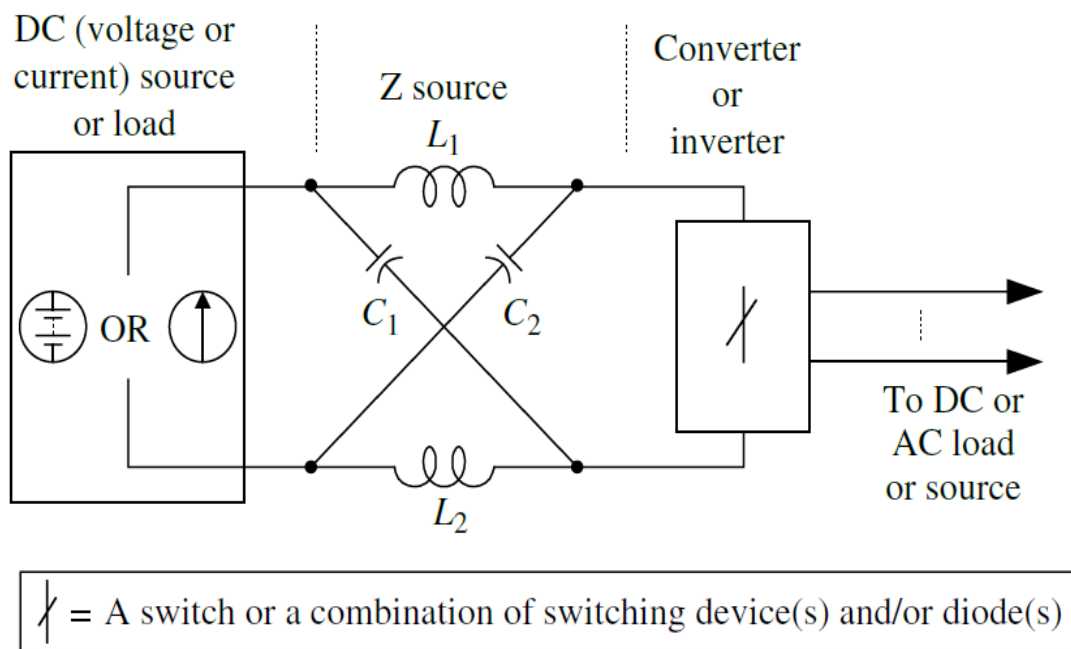
FIGURE 6.9 NORMAL LAYOUT OF THE ZSI

To demonstrate the operating principle, a three phase voltage fed ZSI is employed, as shown in Figure 6.9. Six active states and two zero states make up a typical three-phase voltage source inverter. Gating on both the upper and lower devices of any one phase leg, any two phase legs, or all three phase legs of the ZSI allows for multiple additional zero states [69]. These shoot through zero states are forbidden in a normal

voltage source inverter because they would induce short-circuiting across the source. The inverter's buck–boost capability is made possible via the ZSN and shoot through zero states. All traditional pulse width modulation (PWM) techniques can regulate the Zsource inverter, and its theoretical input–output relationships still apply. As a result of the unique attribute of the shoot through zero states, several novel PWM schemes have been developed, such as simple boost type control, maximum boost type control, maximum constant boost type control, and space vector modulation [69-78].
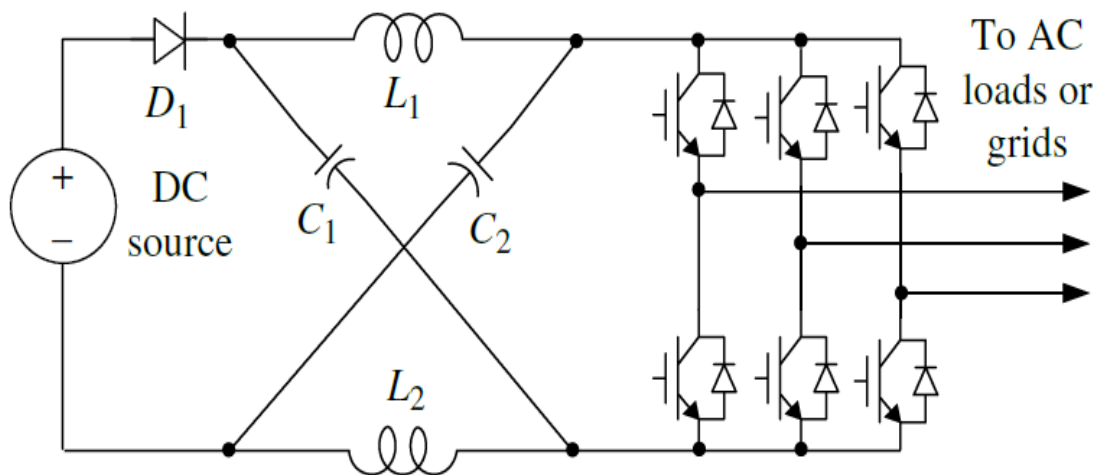
FIGURE 6.10 THREE-PHASE VOLTAGE- SUPPLIED ZSI

6.3.1 Background And Benefits In Contrast With. Current Technology

As previously stated, field of power electronics is the authorizing technology for the energy processing required by all forms of electronic and electrical equipment, from renewable energy to power systems, from household appliances to aircraft systems. Both the VS and CS converters have the following three common conceptual and theoretical constraints that preclude them from being used in many applications.

i. They can only be a boost or a buck converter. As a result, the range of possible output voltages is either lower or higher than the input voltage.

ii. It is not possible to swap their primary circuits. To put it another way, the VS converter's main circuit cannot be used as a CS converter or vice versa.

iii. They are susceptible to EMI noise, making them less reliable than expected.

Unlike the standard VS or CS, the Z SI can be open and shortcircuited, allowing the main converter circuit to step up or down the voltage as needed. For the source, main circuit, and load, the ZSI offers the following three levels of flexibility:

i. A voltage or current source can be used to power the ZSI. Unlike standard VS or CS converters, the ZSI's dc source examples are a battery, diode rectifier, thyristor converter.

ii. The ZSI's primary circuit can be VS or CS. Furthermore, switches in the ZSI can be a combination of switching devices and diodes, as shown in Figures 6.10 and 6.11.

iii. Inductive or capacitive loads can be used with the ZSI.
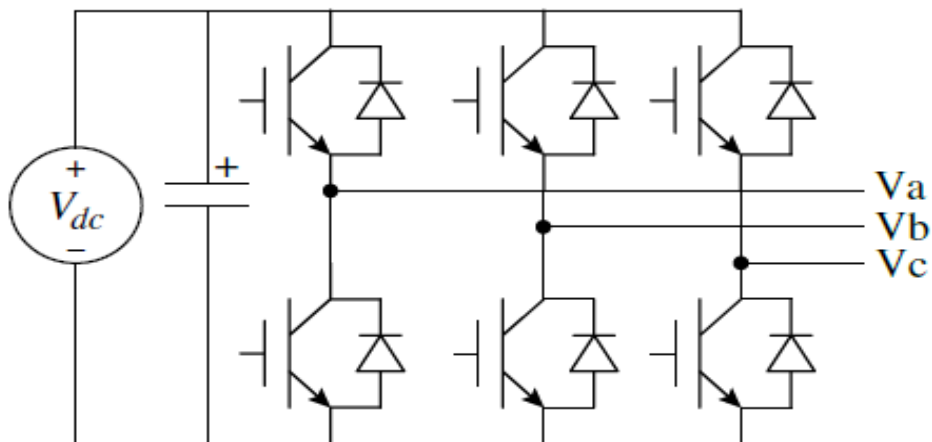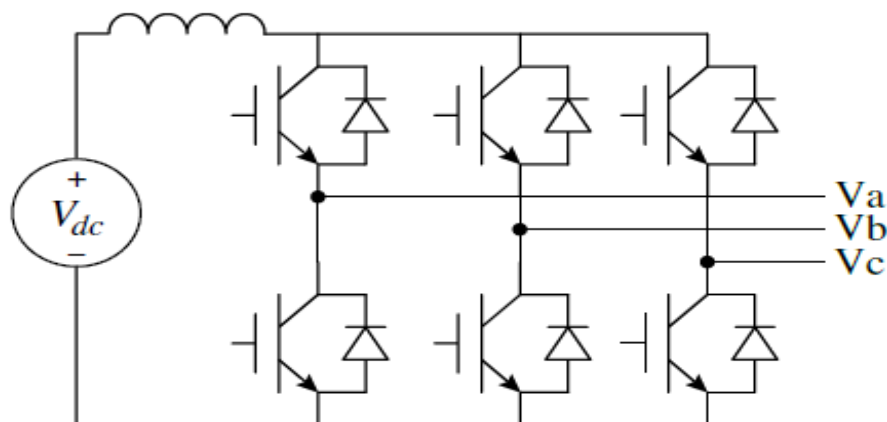

FIGURE 6.11 TYPICAL DC-AC VOLTAGE-SOURCE CONVERTER

FIGURE 6.12 TYPICAL DC-AC CURRENT-SOURCE CONVERTER

6.3.2 Present Status And Classification

Unlike the usual Voltage Source or Current Source, the ZSN can opearte in an open as well as in short circuit condition both, facilitating the principal converter circuit to boost and buck voltage as & when required for achieving power conversion in one step. These attributes allow the ZSI to execute the same operation with respect to a traditional two-step converter or inverter, also with fewer components and at a cheaper cost. Dead time is eliminated, resulting in better output current/voltage waveform quality (no distortion). All dc-ac, ac-dc, ac-ac, and dc-dc converter power conversions have been included in the Z-source concept [79, 80].

PV power generating [81-87], wind power generation [88-95], electric cars [96-100], and so on are some of the application domains that are involved. Following on from the VS and CS converters, the ZSI has unquestionably been a key branch of power electronic converters.

Since its inception, study into Zsource has been a hot issue. The number of new Zsource topologies and modifications has skyrocketed. A summary of ZSI categories and Zsource network topologies reported in recent literature is shown in Figure 6.12(a) and (b). Ac-dc rectifiers, dc-ac inverters, ac-ac converters, and dc-dc converters are the four primary groups based on conversion capabilities. Two and multilevel [69-78, 81-87], ac-ac regulators [102-106], matrix converters [107-113], and nonisolated and isolated dc-dc converters [114-118] are the results of a further breakdown. It can be voltage fed or current fed from a ZSN topology standpoint.

Amending the original Z-source network, or shuffling the connections of inductors and capacitors, resulted into the developmemt of various ZSN topologies. For diverse or specific application demands, each Z-source network topology has its own unique features.

(a)

(b)
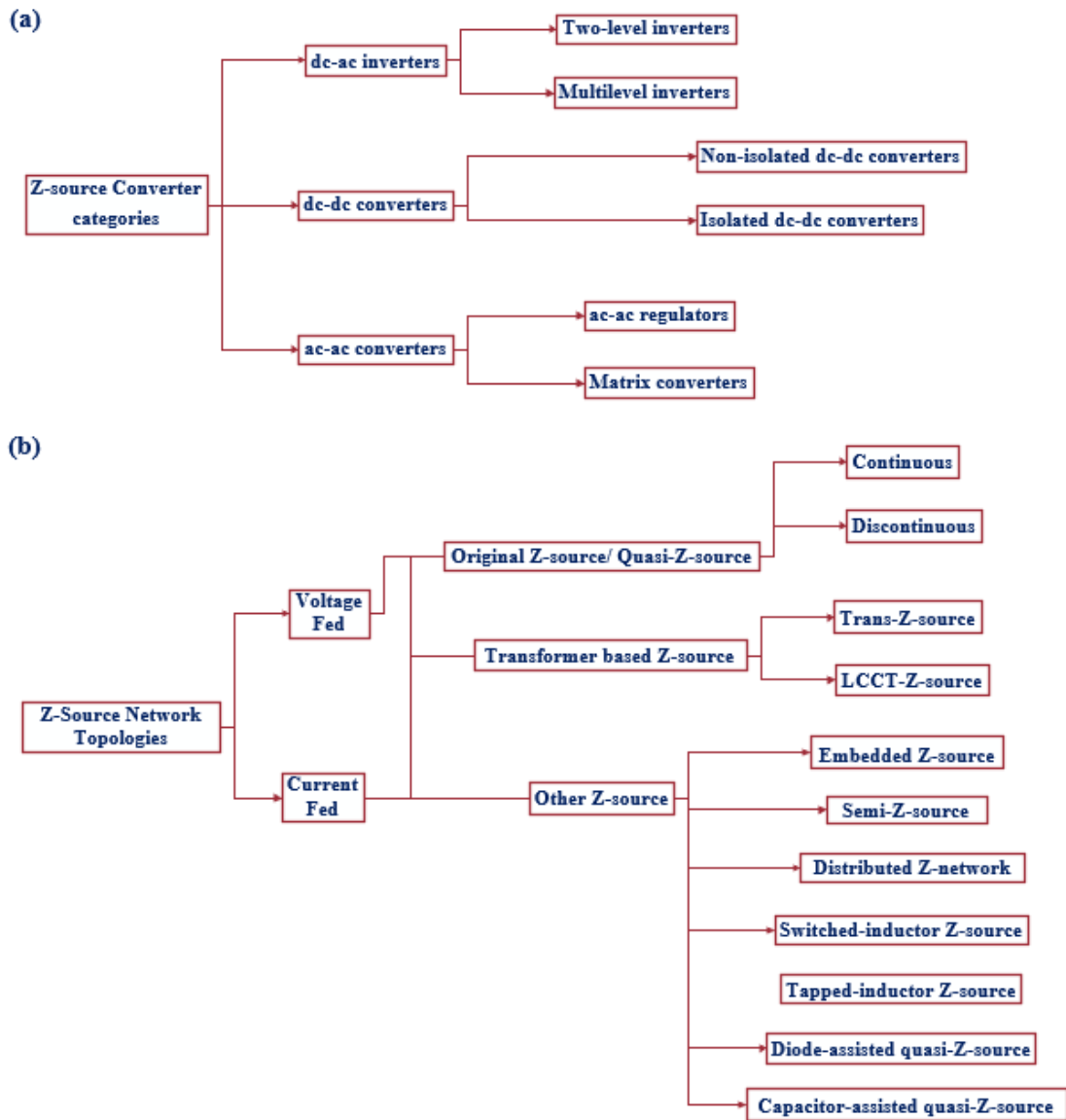
FIGURE 6.13 SUMMARY OF DIFFERENT Z-SOURCE CONVERTERS: (A) CATEGORIZATIONS OF Z-SOURCE CONVERTERS; (B) TOPOLOGIES OF Z-SOURCE INVERTERS.

Three factors are driving the development of new ZSI topologies:

i. count and rating of ZSI components

ii. voltage gain range expansion

iii. Optimization and enhancement of applications

   Quasi ZSI find its application in renewable power production and vehicle driving applications. The embedded type ZSI multisource capability makes it appropriate for photovoltaic power generation. The voltage gain of the original Z-

source, quasi Z-source, and embedded Z-source is theoretically limitless. However, if the voltage gain is high (>2–3), the switches will be subjected to a lot of voltage stress. Trans type ZSI facilitates larger gain in Voltage while also using less components (only one transformer/inductor & capacitor). Various extensions to Quasi Type ZSI provide many different ways to boost voltage gain, but they require more components. For single phase grid tie PV power systems requirements, semi ZSIs have been developed to achieve cheap cost and high efficiency. A voltage boost function and a double ground feature in a semi Z-source type inverter containing only two switches operating in active mode minimise the requirement to float/isolate PV panels without leakage current, improving safety. A ZSN can be built out of distributed impedance networks like transmission lines and hybrid LC components. Although these distributed ZSNs are challenging to design, a distributed ZSI requires no additional diode or switch to provide the voltage boost function, resulting in a low component count.

6.4 LLC RESONANT CONVERTER

A full-Bridge LLC resonant DC-DC converter is shown in Figure 6.13 with resonant capacitor C_r, resonant inductor L_r and magnetizing inductor L_m. It has three components as follows:

i.   Square Wave generator:

Power switches Q1, Q2, Q3, Q4, which are generally MOSFETs, are arranged to form a square wave generator. This generator yields a bipolar square-wave voltage (V_{sw}) by driving switches Q1 and Q4 & Q2 and Q3 alternately with pulse frequency modulation approach that uses a variable frequency clock to drive the power switches and transfer energy from the input to the output.

ii. Resonant Network:

Resonant capacitor C_r, resonant inductor L_r, and magnetising inductor L_m comprise the resonant network. The resonant network circulates the energy and delivers it to the load via the transformer. A bipolar square wave is received at the transformer's primary side and passed via the secondary winding. Electrical isolation is also provided by the transformer, as well as the required turn ratio for the required output voltage.

iii. Rectifier Network:

The rectifier network converts AC voltage to DC voltage using diodes and capacitors. The rectifier network is made up of a complete bridge rectifier with a capacitive output filter.
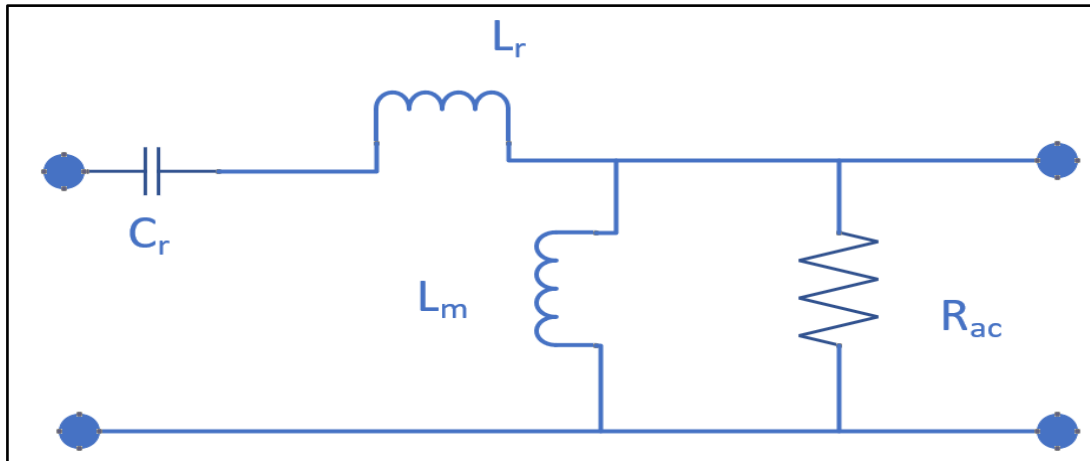

FIGURE 6.14 EQUIVALENT MODEL OF LLC RESONANT CONVERTER

CHAPTER 7

DESIGN & CONTROL OF Z-SOURCE BASED RESONANT CONVERTER

7.1 GENERAL

In comparison to DC/AC applications, Z-Source Resonant Converters have more states in a single switching cycle. All such states must be elucidated in order to perceive the ZSRC. Amidst such states, the boost type ratio of the Z-Source Inverter is still influenced by and large by the shoot through state duty cycle. The upcoming section explains the ZSRC operation principle.

7.2 ZSRC BCS SYSTEM OPERATION PRINCIPLE

For conventional analysis, the AC voltage source and input rectifier were processed as a DC voltage source with a value of |Vac| (absolute value of AC input voltage), as illustrated in Figure 7.1. Considered the fact that the resonant network serves as a type of filter permitting the current lying within a certain range or band of frequencies to pass, thereby flowing current at the resonant frequency only. Assuming, that the Z-Source Inverter (ZSI) components in Fig. 7.1 are symmetrical ($C_1 = C_2 = C$ and $L_1 = L_2 = L$), we have: $V_{C1} = V_{C2} = V_C$ and $V_{L1} = V_{L2} = V_L$. Furthermore, ZSN's switching frequency is ten times lower than L and C's resonant frequency. As a result, for a single switching cycle, the Z-Source Inverter (ZSI) inductor current and Z-Source Inverter (ZSI) capacitor voltage are deemed steady.

The principal output factor of the H-bridge type inverter topology is in coherence with the current at primary end (i_{rp}) of LLC Resonant Converter at resonance frequency [40], and the overall duration of shoot through period (T_{st}) is uniformly disseminated throughout one switching period.
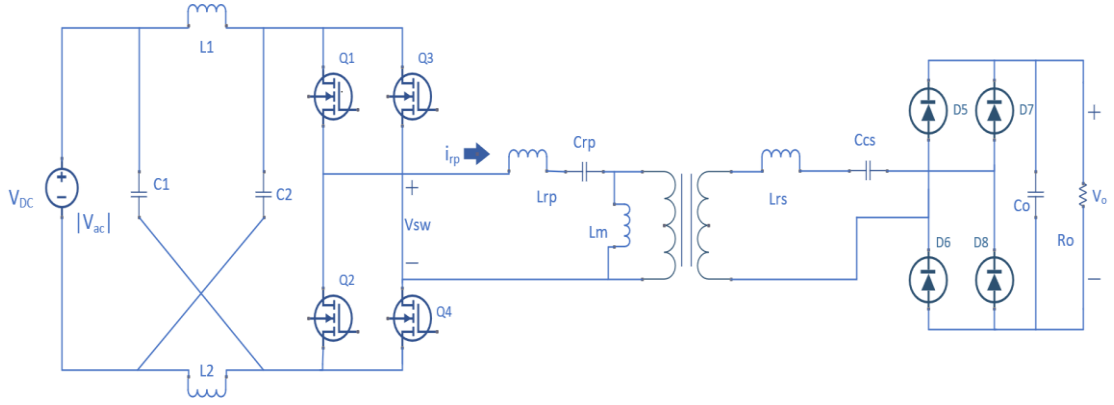
FIGURE 7.1 EQUIVALENT DC MODEL OF ZSRC

7.3 Z-SOURCE DESIGN PARAMETERS

The determination of values for the reactive components of the impedance network is the most problematic aspect of ZSI design. The component values should be assessed for the converter's minimal input voltage, where the boost factor and current stresses are at their highest.

i. Inductor current average calculation:

$$I_L = P/V_{DC} \qquad (7.1)$$

When maximum shoot-through occurs, maximum ripple current is generated. If ΔI_L is the inductor's maximum ripple current, then:

$$\Delta I_L = I_{Lmax} - I_{Lmin} \qquad (7.2)$$

Where I_{Lmax} & I_{Lmin} are the maximum & minimum values of inductor current respectively.

ii. The Boost Factor of the input voltage is:

$$B = \frac{1}{\left(1 - 2D_Z\right)} = \frac{V_{DC1}}{V_{DC}} \qquad (7.3)$$

iii. Shoot through state Duty Cycle is given by:

$$D_{st} = \frac{B-1}{2B} \qquad (7.4)$$

iv. Z-Source Capacitor Voltage is given by:

$$V_C = \frac{V_{DC} + V_{DC1}}{2} \qquad (7.5)$$

v. Calculation of required value of Z-Source Inductance is given by:

$$L = \frac{T_{st} \cdot V_C}{\Delta I_L} \qquad (7.6)$$

vi. Shoot-Through period per switching cycle is given by:

$$T_{st} = \frac{D_{st}}{T} \qquad (7.7)$$

vii. Calculation of required value of Z-source Capacitance is given by:

$$C = \frac{I_L * T_{st}}{\Delta V_C} \qquad (7.8)$$

Where ΔV_c is the Voltage ripple across the Z-Source Capacitor.

7.4 DIFFERENT STATES OF ZSRC

In contrast with DC/AC applications, ZSI has more states per switching interval. All of these states must be understood in order to understand the ZSRC. Active, Shoot Through, and Zero are these three states.

All of ZSRC's conceivable states are represented by these three states. Varying load regulation characteristics would result from different allocations of these three states during the course of a switching period.

i. Active State:

The diagonal switches are ON. Both the ZSN inductor and the capacitor supply current to the resonant network. The dissimilarity amid load current (i_{rp}) and ZSN inductor current is originated by connecting the two ZSN capacitors in series with the DC source (I_L). Only load current travels via the switches (i_{rp}). For this time interval, the ZSN inductor voltage is as follows:

$$V_L = 0.5\left(|V_{ac}| - V_z\right) = 0.5\left(\left|\widehat{V_{ac}}\sin \omega t\right| - V_z\right) \qquad (7.9)$$

Where $\widehat{v}_{ac}$ is the AC input voltage maximum value and ω is the line's angular frequency.

ii. Shoot Through State:

Three switches are turned on. The load current is carried by two horizontal switches, while the Z-Source Inverter (ZSI) inductor current is carried by two switches in one phase leg. As a result, the two currents are carried by a single switch. Because the ZSN current of inductor is always unipolar and the current of load is bidirectional, these two currents whether subtract or add, assisting to the sum with their definite values. In the shoot through state, phase shift based control mechansim permits only various polarity currents to pass through the same switch. The ZSN capacitors charge the ZSN inductors here (this is how the Z-Source Resonance Circuit may enhance the voltage). For this time interval, the Z-Source Network inductor voltage is as follows:

$$V_L = V_C \qquad (7.10)$$

iii. Zero State:

Two horizontal switches are ON during the time interval of zero state. The Z-Source Network is not connected to the load in any way. The load current is freewheeling, and the Z-Source Network capacitors are charged by the inductors. For this time interval, the ZSN inductors' voltage is represented as:

$$V_L = V_{DC} - V_C \qquad (7.11)$$

Using voltage second balance across the ZSN inductor throughout one switching period by combining Equation (7.1), (7.2), and (7.3), we have:

$$\frac{T_{act}}{T_s}\left(V_{DC} - V_C\right) + \frac{T_{st}}{T_S}V_C + \left(1 - \frac{T_{act}}{T_S} - \frac{T_{st}}{T_S}\right)\left(V_{DC} - V_C\right) = 0 \tag{7.12}$$

$$V_C = \frac{1 - D_{st}}{1 - 2D_{st}}V_{DC} \tag{7.13}$$

$$D_{st} = \frac{V_Z - V_{DC}}{2V_Z} = \frac{V_C - V_{DC}}{2V_C - V_{DC}} \tag{7.14}$$

$$V_Z = \frac{V_{DC}}{1 - 2D_{st}} \tag{7.15}$$

The PFC is governed by the shoot-through duty cycle, which is another control variable in the system. $D_{act} + D_{st} + D_{zer} = 1$ should always be met by its management, where $D_{zer} = \frac{T_{zer}}{T_s}$ is the conventional zero state duty cycle.

According to this relationship in Equation (7.6), the voltage on the ZSN capacitor is unrelated to the active state duty cycle D_{act}.

TABLE 7.1 SWITCH SELECTION DURING DIFFERENT STATES

STATES	INVERTER SWITCHES ON
ZERO	Q2,Q4 or Q1,Q3
SHOOT THROUGH	Q1,Q2,Q4 or Q1,Q3,Q4 or Q1,Q2,Q3 or Q2,Q3,Q4
ACTIVE	Q1,Q4 or Q2,Q3

CHAPTER 8

RESULTS AND DISCUSSIONS

8.1 GENERAL

The simulation parameters and component values are listed in Table 8.1 & Table 8.2. The ZSN design was based on [50, 63] and was targeted at decreasing the twice-line frequency ripple (twice ripple) passing through it. The SRC design, on the other hand, was inspired by [51, 52], with compensating capacitors adjusted so that the band pass filter's resonance frequency was equal to the switching frequency. These systems have switching frequencies ranging from 100 to 130 kHz [53]. The frequency of 110 kHz was chosen for this project.

8.2 VALUES OF PARAMETERS & COMPONENT USED IN MATLAB SIMULATION

TABLE 8.1 PARAMETERS VALUES

Parameters	Values
Input Voltage (V_{ac})	220 V RMS
Line Frequency	50 Hz
Switching Frequency(f_{sw})	117 KHz
Resonant Frequency(f_r)	110 KHz
Output Voltage (V_O)	24 V
Output Current (I_O)	8 A
Output Power (P_O)	192 W
Turns Ratio	13.33:1

TABLE 8.2 COMPONENT VALUES

Components	Values
C_1, C_2	0.40 µF
L_1, L_2	7.81 mH
L_{rp}	80 µH
C_{rp}	26.2 nF
L_m	400 µH
C_O	262 µF
R_O	3 Ω

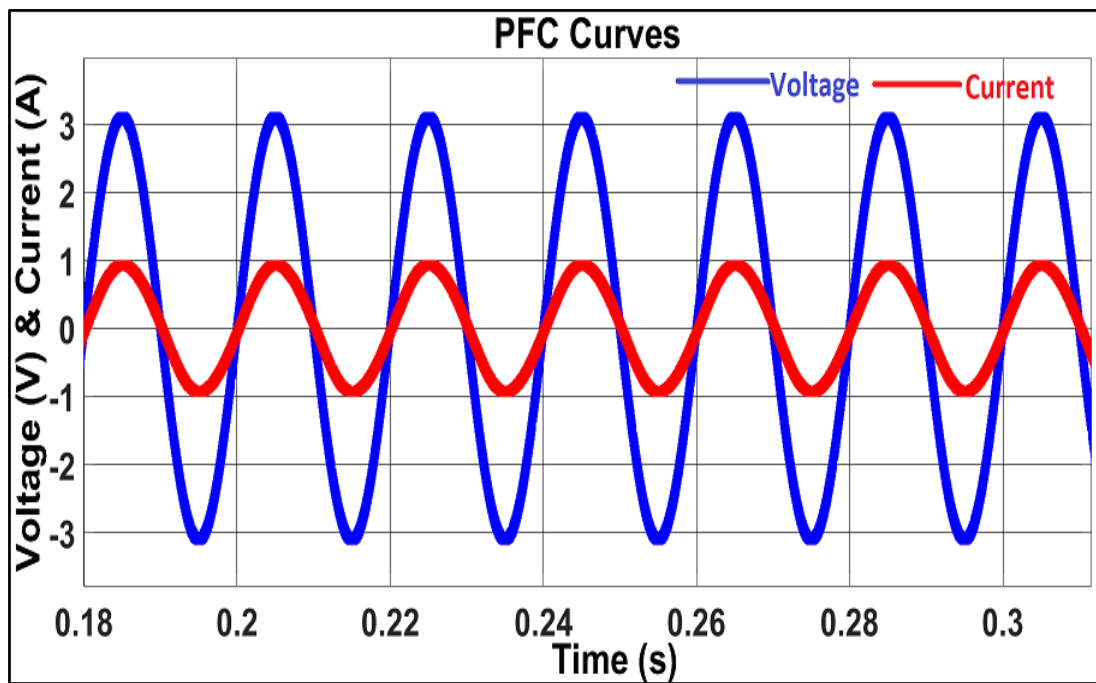## 8.3 WAVEFORMS & RESULTS

FIGURE 8.1 VOLTAGE & CURRENT WAVEFORM SHOWING PFC
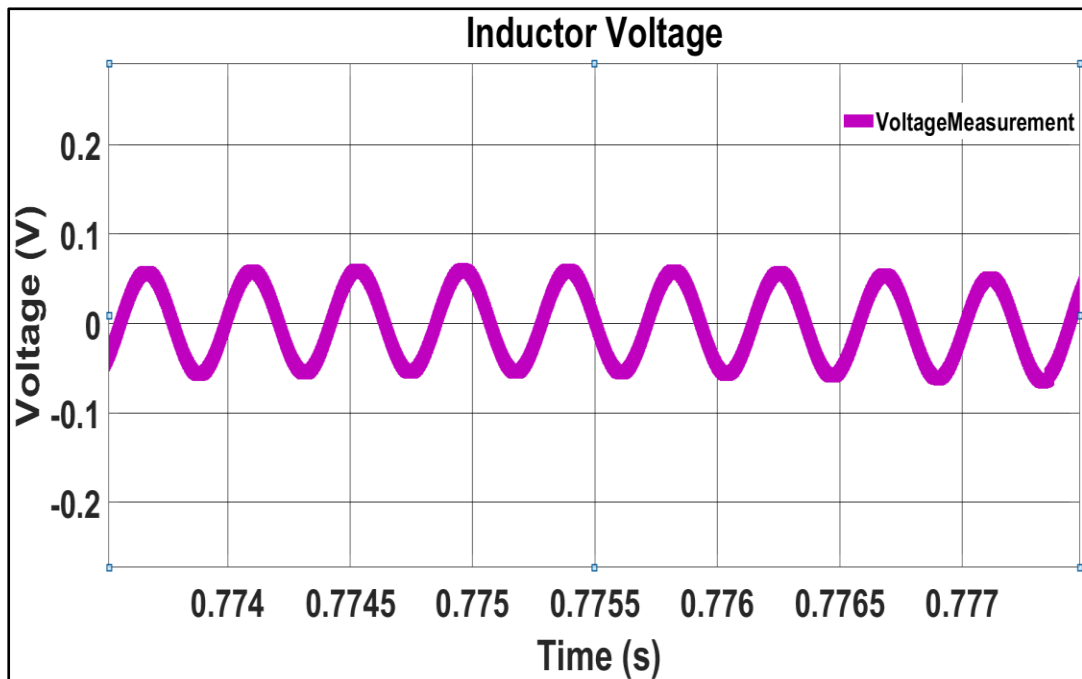
FIGURE 8.2 ZSN INDUCTOR VOLTAGE WAVEFORM
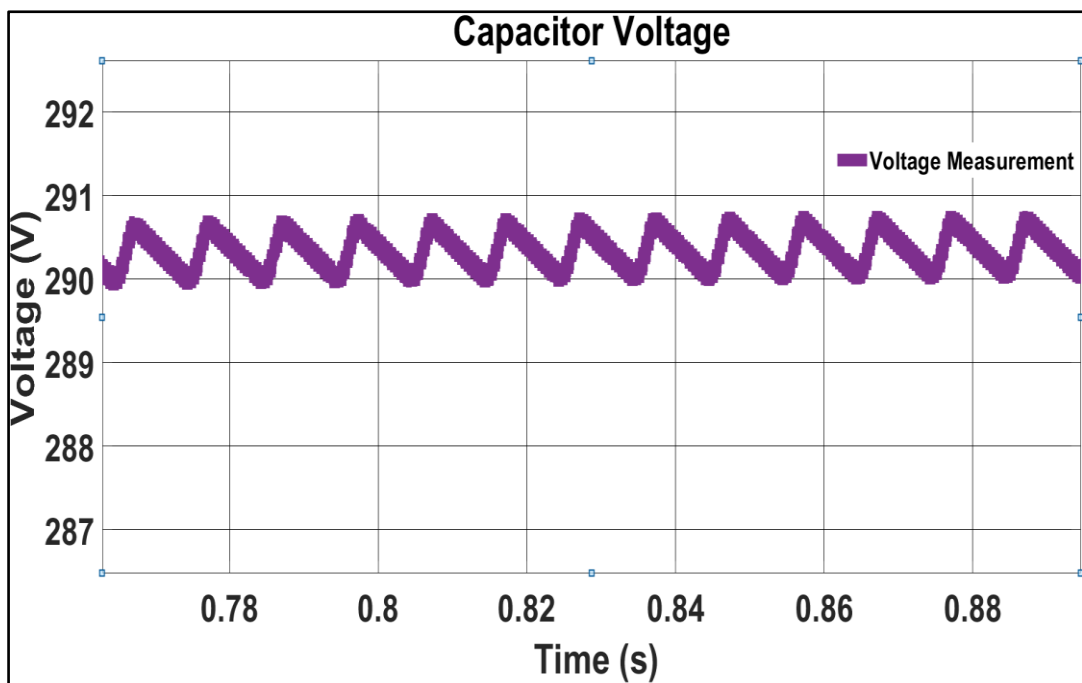
FIGURE 8.3 ZSN CAPACITOR VOLTAGE WAVEFORM
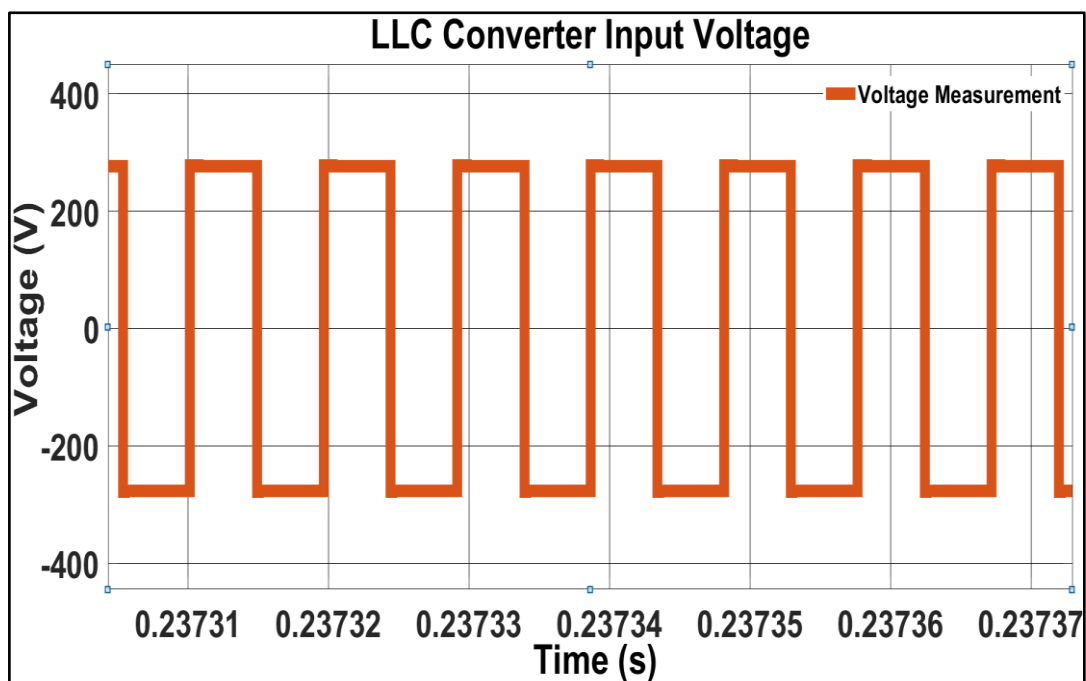
FIGURE 8.4 VOLTAGE WAVEFORM OF LLC RESONANT CONVERTER
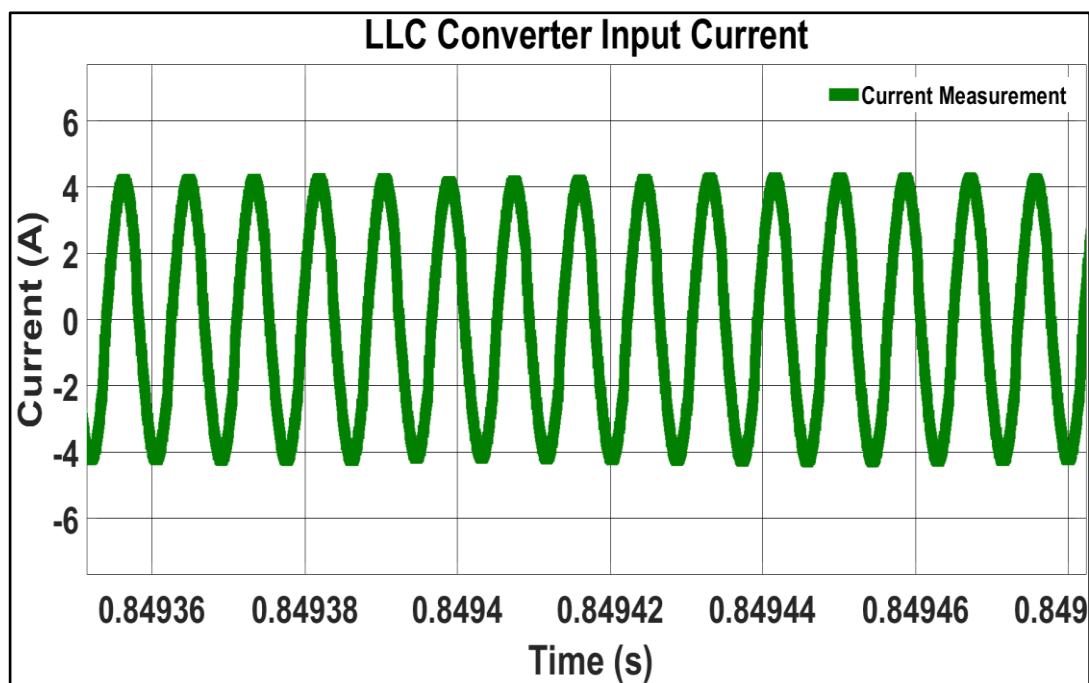
FIGURE 8.5 CURRENT WAVEFORM OF LLC RESONANT CONVERTER
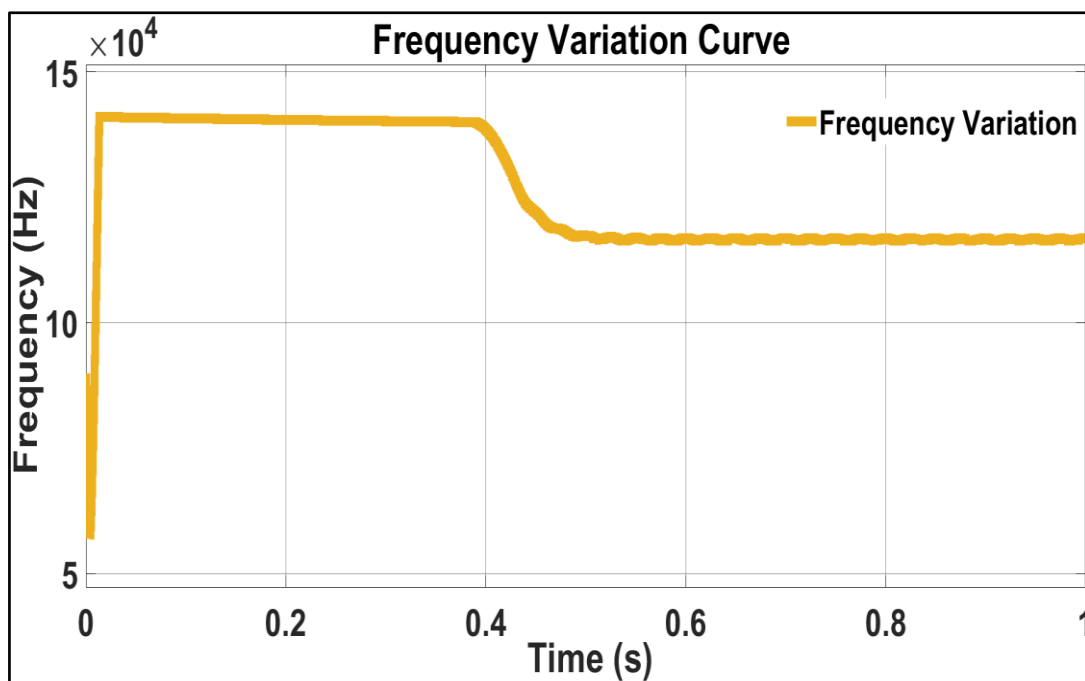
FIGURE 8.6 CURVE SHOWING VARIABLE FREQUENCY OPERATION OF LLC RESONANT CONVERTER
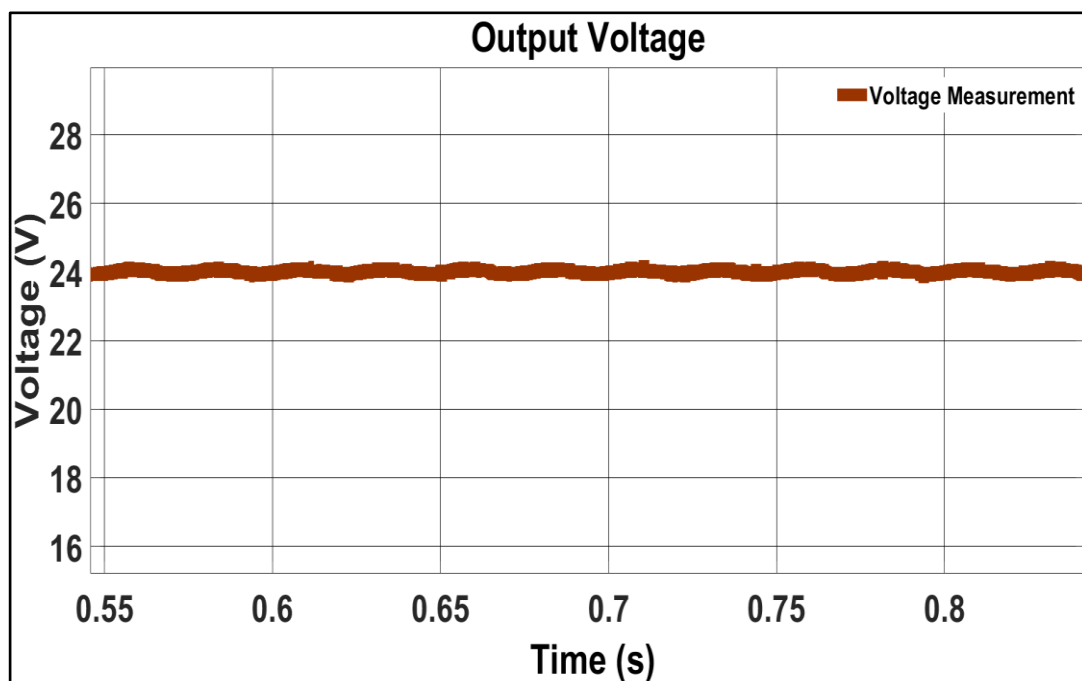
FIGURE 8.7 VOLTAGE WAVEFORM AT THE OUTPUT SIDE
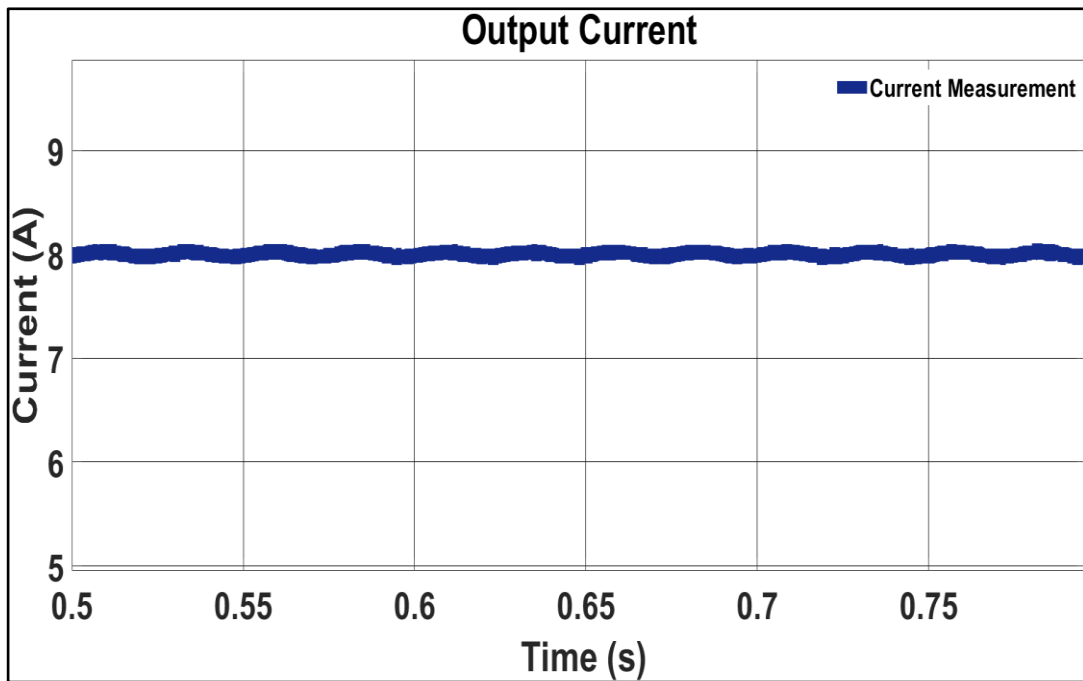
FIGURE 8.8 VOLTAGE WAVEFORM AT THE OUTPUT SIDE

The circuit modelling of ZSRC BCS System have been introduced. The suitable parameters of Switching Frequency (f_{sw}), Transformer Turns Ratio (n), L_n (relationship between the magnetising inducatnce (L_m) and series resonant inductance (L_r)) & Quality Factor (Q_e) have been chosen to create a Full-Bridge LLC Resonant Converter.

Figure 8.1 shows input AC Voltage & Input Current with improved phase response achieving a P.F of almost Unity. Figure 8.2 & Figure 8.3 show Voltage across Z-source inductor & Z-Source capacitor respectively. Figure 8.4 & Figure 8.5 shows Input Voltage & Current across LLC Resonant Converter respectively. Figure 8.6 shows a wide operating switching Frequency Range Operation of an LLC Resonant Converter. Figure 8.7 & Figure 8.8 shows rectified DC Output Voltage & Current respectively.

CHAPTER 9

CONCLUSION AND FUTURE SCOPE

9.1 GENERAL

This project demonstrated the role of ZSN using a Z-Source Resonance Converter for Electic Vehicle Battery charging as an example. The ZSRC is immune to shoot-through states thanks to the ZSN, which not only improves system dependability but also introduces another control parameter (shoot-through state duty cycle) that may be used for Power Factor Correction. The suggested Z-Source Network based On Board Charger was analysed and matched to the standard boost-converter-based OBC in this study.

This project used simulations to validate the theoretical analysis & could be used as an On-Board Battery Charger of 24V & 8A. While regulating the system output voltage to 24V, the suggested single stage PFC converter system obtained a PF of 0.9981 & T.H.D of 1.33%.

9.2 CONCLUSION

Clearly, the ZSI topology has ushered in a modern era of study in the field of power electronics. The preceding explanation is simply a summary of the most common Z-source network topologies. The Z-source topologies have been modified and twisted in several ways. Each topology has its own set of characteristics and uses. There is no single solution that works for everyone. New Z-source topologies may emerge in the future to suit needs and increase performance in various applications.

Because of their unique voltage buck–boost capability with little component count and possibly low cost, ZSIs will find applications in adjustable frequency drives and clean energy generation, such as Photo-Voltaic and Wind Energy.

The performance of ZSIs will undoubtedly be enhanced by new power electronic components such as SiC and GaN. In view of the fact that these components have ultra-high switching frequencies, lesser power loss, and superb thermal capability, count of Z-source passive components required will be lower thereby

converter efficiency will be higher. In terms of topologies and applications, ZSIs are still moving forward.

9.3 FUTURE SCOPE

With reference to the Current Project, future work will include optimising the governing methodology to reduce harmonic content and integrating soft switching to improve system efficiency so as to meet the required standards. Also, while implementing this research study into a hardware model for executing Wireless Power Transmission, we need to use a Mutual Inductor in place of Transformer.

REFERENCES

[1] G. A. Covic and J. T. Boys, "Modern trends in inductive power transfer for transportation applications," IEEE J. Emerging Sel. Topics Power Electron., vol. 1, no. 1, pp. 28–41, Mar. 2013.

[2] N. Tesla, "Apparatus for transmitting electrical energy," US Patent 1 119 732, Dec. 1, 1914.

[3] Grant A. Covic, John T.Boys " Inductive power transfer" in Proc. of the IEEE vol.101, No.6, June 2013.

[4] A. Khaligh and S. Dusmez, "Comprehensive topological analysis of conductive and inductive charging solutions for plug-in electric vehicles," IEEE Trans. Veh. Technol., vol. 61, no. 8, pp. 3475–3489, Oct. 2012

[5] Shigeo Kawasaki,Yuta Kobayashi,Satoshi Yoshida " High-power, high efficiency microwave circuits and modules for wireless power transfer based on green-Eco technology" Proc. of 2013 IEEE Radio and Wireless Symposium.

[6] Ryo Ishikawa; Kazuhiko Honjo "Efficient supply power control by PWM technique for microwave wirelesspower transfer systems" Proc. of 2014 Asia-Pacific Microwave Conference.

[7] Hiroshi Tonomura; Junji Miyakoshi, Naoki Shinohara; "Researches of microwave safety issue of wireless power transfertechnology for commercial vehicles" Proc. of 2015 9th European Conference on Antennas and Propagation (EuCAP).

[8] Naoki Shinohara "Research and standardization activities of wireless power transfer via microwaves at Kyoto university" Proc. of 2015 International Workshop on Antenna Technology (iWAT).

[9] Fariborz musavi, Wilson Eberle "overview of wireless power transfer technologies for electric vehicle battery charging" in proc. In IET Power electronics, 2014, vol.7, Iss.1, pp.60-66.

[10] Kline, M., Izyumin, I., Boser, B., Sanders, S.: "Capacitive power transfer for contactless charging". IEEE Applied Power Electronics Conf. and Exposition (APEC), 2011, pp. 1398–1404.

[11] Liu, C., Hu, A.P., Dai, X.: "A contactless power transfer system with capacitively coupled matrix pad". IEEE Energy Conversion Congress and Exposition (ECCE), 2011, pp. 3488–3494.

[12] Deepak Rozario; Najath Abdul Azeez; Sheldon S. Williamson "Analysis and design of coupling capacitors for contactless capacitivepo wer transfer systems" Proc. Of 2016 IEEE Transportation Electrification Conference and Expo (ITEC).

[13] Chao Liu; Aiguo Patrick Hu; Mickel Budhia "A generalized coupling model for Capacitive Power Transfer systems" Proc. Of IECON 2010 - 36th Annual Conference on IEEE Industrial Electronics Society.

[14] Stanimir Valtchev, Beatriz Borges, Kostadin Brandisky, J.Ben Klaassens " Resonant Contactless energy transfer with improved Efficiency" in proc. IEEE Transactions on power electronics, Vol.24, No.3, March 2009.

[15] Beh, T.C., Imura, T., Kato, M., Hori, Y.: "Basic study of improving efficiency of wireless power transfer via magnetic resonance coupling based on impedance matching". IEEE Int. Symp. on Industrial Electronics (ISIE), 2010, pp. 2011–2016.

[16] Siqi Li and Chunting Chris Mi "Wireless power transfer for electric vehicle applications" in Proc. IEEE journal of emerging and selected topics in power electronics, Vol.3, No.1, March 2015.

[17] W. Zhang, S.-C. Wong, C. K. Tse, and Q. Chen, "Analysis and comparison of secondary series- and parallel-compensated inductive power transfer systems operating for optimal efficiency and loadindependent voltage-transfer ratio," IEEE Trans. Power Electron., vol. 29, no. 6, pp. 2979–2990, Jun. 2014.

[18] Zhong chen, Wuwei Jing, Xueling Huang, Linlin Tan, Chen Chen, Wei Wang " A promoted Design for primary coil in roadway-powered system" Proc. IEEE Transactions on magnetics vol.51, No.11, November 2015.

[19] J. Huh, S. W. Lee, W. Y. Lee, G. H. Cho, and C. T. Rim, "Narrow-width inductive power transfer system for online electrical vehicles," IEEE Trans. Power Electron., vol. 26, no. 12, pp. 3666–3679, Dec. 2011.

[20] S. W. Lee, J. Huh, C. B. Park, N. S. Choi, G. H. Cho, and C. T. Rim, "On-line electric vehicle using inductive power transfer system," IEEE Energy Convers. Congr. Expo., Sep. 2010, pp. 1598–1601.

[21] Yilmaz, M.; Krein, P.T., "Review of Battery Charger Topologies, Charging Power Levels, and Infrastructure for Plug-In Electric and Hybrid Vehicles," in Power Electronics, IEEE Transactions on , vol.28, no.5, pp.2151-2169, May 2013

[22] Modern Trends in Inductive Power Transfer for Transportation Applications- Covic, G.A.; Boys, J.T., "Modern Trends in Inductive Power Transfer for Transportation Applications," in Emerging and Selected Topics in Power Electronics, IEEE Journal of , vol.1, no.1, pp.28-41, March 2013.

[23] Musavi, F.; Edington, M.; Eberle, W., "Wireless power transfer: A survey of EV battery charging technologies," Energy Conversion Congress and Exposition (ECCE), 2012 IEEE, vol., no., pp.1804, 1810, 15-20 Sept. 2012.

[24] Ekemezie, P.N., "Design of a power factor correction ac-dc converter," AFRICON 2007, vol., no., pp.1, 8, 26-28 Sept. 2007.

[25] Rajappan, Suja C.; John, Neetha, "An efficient bridgeless power factor correction boost converter," Intelligent Systems and Control (ISCO), 2013 7th International Conference on , vol., no., pp.55,59, 4-5 Jan. 2013.

[26] Adragna, C.; Huber, L.; Irving, B.T.; Jovanovic, M.M., "Analysis and Performance Evaluation of Interleaved DCM/CCM Boundary Boost PFC Converters Around Zero-Crossing of Line Voltage," in Applied Power Electronics Conference and Exposition, 2009. APEC 2009. Twenty-Fourth Annual IEEE , vol., no., pp.1151-1157, 15-19 Feb. 2009.

[27] Yungtaek Jang; Jovanovic, M.M., "Bridgeless buck PFC rectifier," in Applied Power Electronics Conference and Exposition (APEC), 2010 Twenty-Fifth Annual IEEE , vol., no., pp.23-29, 21-25 Feb. 2010.

[28] Yun-Sung Kim; Won-Yong Sung; Byoung-Kuk Lee, "Comparative Performance Analysis of High Density and Efficiency PFC Topologies," in Power Electronics, IEEE Transactions on , vol.29, no.6, pp.2666-2679, June 2014.

[29] Huber, L.; Liu Gang; Jovanovic, M.M., "Design-Oriented Analysis and Performance Evaluation of Buck PFC Front End," in Power Electronics, IEEE Transactions on , vol.25, no.1, pp.85-94, Jan. 2010.

[30] Jovanovic, M.M.; Yungtaek Jang, "State-of-the-art, single-phase, active power-factor-correction techniques for high-power applications - an overview," in Industrial Electronics, IEEE Transactions on , vol.52, no.3, pp.701-708, June 2005.

[31] Marxgut, C.; Krismer, F.; Bortis, D.; Kolar, J.W., "Ultraflat Interleaved Triangular Current Mode (TCM) Single-Phase PFC Rectifier," in Power Electronics, IEEE Transactions on , vol.29, no.2, pp.873-882, Feb. 2014.

[32] Huber, L.; Irving, B.T.; Jovanovic, M.M., "Effect of Valley Switching and Switching-Frequency Limitation on Line-Current Distortions of DCM/CCM Boundary Boost PFC Converters," in Power Electronics, IEEE Transactions on , vol.24, no.2, pp.339-347, Feb. 2009.

[33] Orabi, M.; Ninomiya, T., "A unified design of single-stage and two-stage PFC converter," in Power Electronics SSpecialist Conference, 2003. PESC '03. 2003 IEEE 34th Annual , vol.4, no., pp.1720-1725 vol.4, 15-19 June 2003.

[34] Zeng, Hulong, and Junming Zhang. "An improved control scheme for buck PFC converter for high efficiency adapter application." Energy Conversion Congress and Exposition (ECCE), 2012 IEEE. IEEE, 2012.

[35] Ghanbari, A.R.; Moghani, J.S.; Abdi, B., "Single-stage soft-switching PFC converter based on DCVM buck and flyback converters," in Power Electronics, Drive Systems and Technologies Conference (PEDSTC), 2013 4th , vol., no., pp.218-223, 13-14 Feb. 2013.

[36] Kwon, J.-M.; Choi, W.-Y.; Do, H.-L.; Kwon, B.-H., "Single-stage half-bridge converter using a coupled-inductor," in Electric Power Applications, IEE Proceedings - , vol.152, no.3, pp.748-756, 6 May 2005.

[37] Zhang Bo; Yang Xu; Xu Ming; Chen Qiaoliang; Wang Zhaoan, "Design of Boost-Flyback Single-Stage PFC converter for LED power supply without electrolytic capacitor for energy-storage," in Power Electronics and Motion Control Conference, 2009. IPEMC '09. IEEE 6th International , vol., no., pp.1668-1671, 17-20 May 2009.

[38] Huber, L.; Jovanovic, M.M., "Design optimization of single-stage single-switch input-current shapers," in Power Electronics, IEEE Transactions on , vol.15, no.1, pp.174-184, Jan 2000.

[39] Shiguo Luo; Weihong Qiu; Wenkai Wu; Batarseh, I., "Flyboost power factor correction cell and a new family of single-stage AC/DC converters," in Power Electronics, IEEE Transactions on , vol.20, no.1, pp.25-34, Jan. 2005.

[40] Zhang, Junming, Hulong Zeng, and Ting Jiang. "A primary-side control scheme for high-power-factor LED driver with TRIAC dimming capability." Power Electronics, IEEE Transactions on 27.11 (2012): 4619-4629.

[41] Lai, C.M.; Shyu, K.K., "A single-stage AC/DC converter based on zero voltage switching LLC resonant topology," in Electric Power Applications, IET , vol.1, no.5, pp.743-752, Sept. 2007.

[42] O'Sullivan, D.L.; Egan, M.G.; Willers, M.J., "A Family of Single-Stage Resonant AC/DC Converters With PFC," in Power Electronics, IEEE Transactions on , vol.24, no.2, pp.398-408, Feb. 2009.

[43] Musavi, F.; Edington, M.; Eberle, W.; Dunford, W.G., "Evaluation and Efficiency Comparison of Front End AC-DC Plug-in Hybrid Charger Topologies," in Smart Grid, IEEE Transactions on , vol.3, no.1, pp.413-421, March 2012.

[44] Chongming Qiao; Smedley, K.M., "A topology survey of single-stage power factor corrector with a boost type input-current-shaper," in Power Electronics, IEEE Transactions on , vol.16, no.3, pp.360-368, May 2001.

[45] Singh, B.; Singh, B.N.; Chandra, A.; Al-Haddad, K.; Pandey, A.; Kothari, D.P., "A review of single-phase improved power quality AC-DC converters," in

Industrial Electronics, IEEE Transactions on , vol.50, no.5, pp.962-981, Oct. 2003.

[46] Frank, W.; Reddig, M.; Schlenk, M., "New control methods for rectifier-less PFC-stages," in Industrial Electronics, 2005. ISIE 2005. Proceedings of the IEEE International Symposium on , vol.2, no., pp.489-493 vol. 2, 20-23 June 2005.

[47] Yungtaek Jang; Jovanovic, M.M., "Interleaved Boost Converter With Intrinsic Voltage-Doubler Characteristic for Universal-Line PFC Front End," in Power Electronics, IEEE Transactions on , vol.22, no.4, pp.1394-1401, July 2007.

[48] Shaoyong Yang; Dawei Xiang; Bryant, A.; Mawby, P.; Ran, L.; Tavner, P., "Condition Monitoring for Device Reliability in Power Electronic Converters: A Review," in Power Electronics, IEEE Transactions on , vol.25, no.11, pp.2734-2752, Nov. 2010.

[49] Yuan Li; Shuai Jiang; Cintron-Rivera, J.G.; Fang Zheng Peng, "Modeling and Control of Quasi-Z-Source Inverter for Distributed Generation Applications," Industrial Electronics, IEEE Transactions on , vol.60, no.4, pp.1532,1541, April 2013.

[50] Miaosen Shen; Joseph, A.; Yi Huang; Peng, F.Z.; Zhaoming Qian, "Design and Development of a 50kW Z-Source Inverter for Fuel Cell Vehicles," in Power Electronics and Motion Control Conference, 2006. IPEMC 2006. CES/IEEE 5th International , vol.2, no., pp.1-5, 14-16 Aug. 2006.

[51] Hulong Zeng; Shuitao Yang; Fangzheng Peng, "Wireless power transfer via harmonic current for electric vehicles application," in Applied Power Electronics Conference and Exposition (APEC), 2015 IEEE , vol., no., pp.592-596, 15-19 March 2015.

[52] Huh, J.; Lee, S.W.; Lee, W.Y.; Cho, G.H.; Rim, C.T., "Narrow-Width Inductive Power Transfer System for Online Electrical Vehicles," in Power Electronics, IEEE Transactions on , vol.26, no.12, pp.3666-3679, Dec. 2011.

[53] A Unity-Power-Factor IPT Pickup for High-Power Applications- Keeling, N.A.; Covic, G.A.; Boys, J.T., "A Unity-Power-Factor IPT Pickup for High-Power Applications," in Industrial Electronics, IEEE Transactions on , vol.57, no.2, pp.744-751, Feb. 2010.

[54] Hung-Chun Chang; Chang-Ming Liaw, "Development of a Compact Switched-Reluctance Motor Drive for EV Propulsion With Voltage-Boosting and PFC Charging Capabilities," in Vehicular Technology, IEEE Transactions on , vol.58, no.7, pp.3198-3215, Sept. 2009.

[55] Yu-Kang Lo; Chung-Yi Lin; Huang-Jen Chiu; Shih-Jen Cheng; Jing-Yuan Lin, "Analysis and Design of a Push–Pull Quasi-Resonant Boost Power Factor Corrector," in Power Electronics, IEEE Transactions on , vol.28, no.1, pp.347-356, Jan. 2013.

[56] Yong-seong Roh; Young-jin Moon; Jeongpyo Park; Changsik Yoo, "A Two-Phase Interleaved Power Factor Correction Boost Converter With a Variation-Tolerant Phase Shifting Technique," in Power Electronics, IEEE Transactions on , vol.29, no.2, pp.1032-1040, Feb. 2014.

[57] Tao Meng; Shuai Yu; Hongqi Ben; Guo Wei, "A Family of Multilevel Passive Clamp Circuits With Coupled Inductor Suitable for Single-Phase Isolated Full-Bridge Boost PFC Converter," in Power Electronics, IEEE Transactions on , vol.29, no.8, pp.4348-4356, Aug. 2014.

[58] Cheng Deng; Min Chen; Pingping Chen; Changsheng Hu; Wenping Zhang; Dehong Xu, "A PFC Converter With Novel Integration of Both the EMI Filter

and Boost Inductor," in Power Electronics, IEEE Transactions on , vol.29, no.9, pp.4485-4489, Sept. 2014.

[59] Vyshakh, A.P.; Unni, M.R., "Performance enhanced BLIL PFC boost converter for PHEV battery chargers," in Emerging Research Areas: Magnetics, Machines and Drives (AICERA/iCMMD), 2014 Annual International Conference on , vol., no., pp.1-6, 24-26 July 2014.

[60] Cha, Honnyong, Fang Z. Peng, and DongWook Yoo. "Z-source resonant DC-DC converter for wide input voltage and load variation." Power Electronics Conference (IPEC), 2010 International. IEEE, 2010.

[61] Laouamri, K.; Ferrieux, J.-P.; Catellani, S.; Barbaroux, J., "Modeling and analysis of wound integrated LCT structure for single stage resonant PFC rectifier," in Power Electronics, IEEE Transactions on , vol.18, no.1, pp.256-269, Jan 2003.

[62] Fang Zheng Peng, "Z-source inverter," Industry Applications, IEEE Transactions on , vol.39, no.2, pp.504,510, Mar/Apr 2003.

[63] M. Shen. "Z-source inverter design, analysis, and its application in fuel cell vehicles." Ph.D. dissertation, Michigan State University, East Lansing, Michigan, 2006.

[64] Ahmed Al Mansur, Abdullah Al Bashit, A.S.M Mahfuzur Rahman,Md.Shahinur Alam, Hasina Begum"Improvement of input side current of a single phase rectifier with variable output voltage range using Boost converter and investigation of harmonic mitigation" ,IJSER,Vol-4, Issue-3, march-2013.

[65] Sudeep PyaKuryal, Md.Matin, " Filter design for AC to DC Converter,IRJES, Vol-2,Issue-6 ,June-2013, PP-42-49.

[66] H Z Azazi, EL-Kohly, S A Mahmoud, S S Shokralla,"Review of Active and Passive circuits for power factor correction in single phase low power DC Converter", Proceedings of 14th MEPCON , 2010.

[67] Suma Umesh, L Venkatesha, Usha A, "Active power factor Correction Technique for Single phase Full Bridge Rectifier", IEEE-ICAECT, 2014.

[68] R Balamurugan, Dr.G Guruswamy, "Harmonic optimization by Single phase improved Power quality AC-DC Power Factor Corrected Converter ", Vol-1, Internation Journal on computer application, 2010.

[69] F. Z. Peng, "Z-Source Inverter," IEEE Trans. Ind. Appl., vol.39, no.2, pp.504–510, March/April 2003.

[70] F. Z. Peng, M. Shen, Z. Qian, "Maximum boost control of the Z-source inverter," IEEE Trans. Power Electron., vol.20, no.4, pp.833–838, July 2005.

[71] M. Shen, J. Wang, A. Joseph, F. Z. Peng, Tolbert L. M., Adams D. J., "Constant boost control of the Z-source inverter to minimize current ripple and voltage stress," IEEE Trans. Ind. Appl., vol.42, no.3, pp.770–778, May–Jun 2006.

[72] Y. Liu, B. Ge, F. J. T. E. Ferreira, A. T. de Almeida, H. Abu-Rub, "Modeling and SVM control of quasi-Z-source inverter," in Proc. 11th International Conference on Electrical Power Quality and Utilisation (EPQU), 2011, pp.1–7.

[73] Y. Tang, S. Xie, J. Ding, "Pulse-width Modulation of Z-Source Inverters With Minimum Inductor Current Ripple," IEEE Trans. Ind. Electron., vol.61, pp.98–106, 2014.

[74] J. Jung, A. Keyhani, "Control of a fuel cell based Z-source converter," IEEE Trans. Energy Convers., vol.22, no.2, pp.467–476, June 2007.

[75] U. S. Ali, V. Kamaraj, "A novel space vector PWM for Z-source inverter," in Proc. 2011 1st International Conference on Electrical Energy Systems (ICEES), 2011, pp.82–85.

[76] H. Rostami, D. A. Khaburi, "Voltage gain comparison of different control methods of the Z-source inverter," in Proc. International Conference on Electrical and Electronics Engineering (ELECO), 2009, pp.I-268–I-272.

[77] O. Ellabban, J. Van Mierlo, P. Lataire, "Experimental study of the shoot-through boost control methods for the Z-source inverter," European Power Electronics and Drives Association Journal, vol.21, no.2, pp.18–29, June 2011.

[78] Y. Liu, B. Ge, H. Abu-Rub, F. Z. Peng, "Overview of Space Vector Modulations for Three-phase Z-Source/Quasi-Z-Source Inverters," IEEE Trans. Power Electron., vol.29, no.4, pp.2098–2108, April 2014.

[79] Y. Liu, H. Abu-Rub, B. Ge, "Z-Source/Quasi-Z-Source Inverters – Derived Networks, Modulations, Controls, and Emerging Applications to Photovoltaic Conversion," IEEE Ind. Electron. Mag., vol.8, no.4, pp.32–44, Dec. 2014.

[80] Y. P. Siwakoti, F. Z. Peng, F. Blaabjerg, P. C. Loh, G. E. Town, "Impedance-Source Networks for Electric Power Conversion Part I: A Topological Review," IEEE Trans. Power Electron., vol.30, no.2, pp.699–716, Feb. 2015.

[81] L. Liu, H. Li, Y. Zhao, X. He, Z. J. Shen, "1 MHz cascaded Z-source inverters for scalable grid-interactive photovoltaic (PV) applications using GaN device," in Proc. 2011 IEEE Energy Conversion Congress and Exposition (ECCE), pp.2738–2745, 2011.

[82] Y. Zhou, L. Liu, H. Li, "A High-Performance Photovoltaic Module-Integrated Converter (MIC) Based on Cascaded Quasi-Z-Source Inverters (qZSI) Using eGaN FETs," IEEE Trans. Power Electron., vol.28, no.6, pp.2727–2738, June 2013.

[83] D. Sun, B. Ge, F. Z. Peng, H. Abu-Rub, D. Bi, Y. Liu, "A New Grid-Connected PV System Based on Cascaded H-bridge Quasi-Z Source Inverter," in Proc. 2012 IEEE International Symposium on Industrial Electronics (ISIE), pp.951–956, 2012.

[84] Y. Fayyad, L. Ben-Brahim, "Multilevel cascaded Z source inverter for PV power generation system," in Proc. 2012 International Conference on Renewable Energy Research and Applications (ICRERA), pp.1–6, 2012.

[85] Y. Liu, B. Ge, H. Abu-Rub, F. Z. Peng, "A Modular Multilevel Space Vector Modulation for Photovoltaic Quasi-Z-Source Cascade Multilevel Inverters", in Proc. 2013 Twenty-Eighth Annual IEEE Applied Power Electronics Conference and Exposition (APEC), pp.714–718, 2013.

[86] Y. Liu, B. Ge, H. Abu-Rub, F. Z. Peng, "An Effective Control Method for Quasi-Z-Source Cascade Multilevel Inverter-based Grid-tie Single-Phase Photovoltaic Power System", IEEE Trans. Ind. Informat., vol.10, no.1, pp.399–407, Feb. 2014.

[87] Y. Xue, B. Ge, F. Z. Peng, "Reliability, Efficiency, and Cost Comparisons of MW Scale Photovoltaic Inverters," in Proc. IEEE Energy Conversion Congress and Exposition (ECCE), pp.1627–1634, 2012.

[88] S. Qu, W. Yongyu, "On control strategy of Z-source inverter for grid integration of direct-driven wind power generator," in 31st Chinese Control Conference (CCC), pp.6720–6723, 25–27 July 2012.

[89] X. Wang, D. M. Vilathgamuwa, K. J. Tseng, C. J. Gajanayake, "Controller design for variable-speed permanent magnet wind turbine generators interfaced with Z-source inverter," in Proc. International Conference on Power Electronics and Drive Systems (PEDS), pp.752–757, 2009.

[90] S. M. Dehghan, M. Mohamadian, A. Y. Varjani, "A New Variable-Speed Wind Energy Conversion System Using Permanent-Magnet Synchronous Generator

and Z-Source Inverter," IEEE Trans. Energy Convers., vol.24, no.3, pp.714–724, Sept. 2009.

[91] U. Supatti, F. Z. Peng, "Z-source inverter with grid connected for wind power system," in Proc. 2009 IEEE Energy Conversion Congress and Exposition (ECCE), pp.398–403, 2009.

[92] T. Maity, H. Prasad, V. R. Babu, "Study of the suitability of recently proposed quasi Z-source inverter for wind power conversion," in Proc. 2014 International Conference on Renewable Energy Research and Application (ICRERA), pp.837–841, 2014.

[93] W.-T. Franke, M. Mohr, F. W. Fuchs, "Comparison of a Z-source inverter and a voltage-source inverter linked with a DC/DC-boost-converter for wind turbines concerning their efficiency and installed semiconductor power," in Proc. 2008 IEEE Power Electronics Specialists Conference (PESC), pp.1814–1820, 2008.

[94] Y. Liu, B. Ge, F. Z. Peng, H. Abu-Rub, A. T. De Almeida, F. J. T. E. Ferreira, "Quasi-Z-Source inverter based PMSG wind power generation system," in Proc. 2011 IEEE Energy Conversion Congress and Exposition (ECCE), pp.291–297, 2011.

[95] B. K. Ramasamy, A. Palaniappan, S. M. Yakoh, "Direct-drive low-speed wind energy conversion system incorporating axial-type permanent magnet generator and Z-source inverter with sensorless maximum power point tracking controller," IET Renewable Power Generation, vol.7, no.3, pp.284–295, May 2013.

[96] F. Z. Peng, M. Shen, K. Holland, "Application of Z-Source Inverter for Traction Drive of Fuel Cell—Battery Hybrid Electric Vehicles," IEEE Trans. Power Electron., vol.22, no.3, pp.1054–1061, May 2007.

[97] S. M. Dehghan, M. Mohamadian, A. Yazdian, "Hybrid Electric Vehicle Based on Bidirectional Z-Source Nine-Switch Inverter," IEEE Trans. Veh. Commun., vol.59, no.6, pp.2641–2653, July 2010.

[98] F. Guo, L. Fu, C. Lin, C. Li, W. Choi, J. Wang, "Development of an 85-kW Bidirectional Quasi-Z-Source Inverter With DC-Link Feed-Forward Compensation for Electric Vehicle Applications," IEEE Trans. Power Electron., vol.28, no.12, pp.5477–5488, Dec. 2013.

[99] P. Liu, H. P. Liu, "Permanent-magnet synchronous motor drive system for electric vehicles using bidirectional Z-source inverter," IET Electrical Systems in Transportation, vol.2, no.4, pp.178–185, December 2012.

[100] Q. Lei, D. Cao, F. Z. Peng, "Novel Loss and Harmonic Minimized Vector Modulation for a Current-Fed Quasi-Z-Source Inverter in HEV Motor Drive Application," IEEE Trans. Power Electron., vol.29, no.3, pp.1344–1357, March 2014.

[101] X. Fang, Z. Qian, F. Z. Peng, "Single-phase Z-source PWM AC-AC converters," IEEE Power Electron Lett., vol.3, no.4, pp.121–124, Dec. 2005.

[102] Y. Tang, S. Xie, C. Zhang, "Z-Source AC-AC Converters Solving Commutation Problem," IEEE Trans. Power Electron., vol.22, no.6, pp.2146–2154, Nov. 2007.

[103] M. Nguyen, Y. Jung, Y. Lim, "Single-Phase AC-AC Converter Based on Quasi-Z-Source Topology," IEEE Trans. Power Electron., vol.25, no.8, pp.2200–2210, Aug. 2010.

[104] L. He, S. Duan, F. Z. Peng, "Safe-Commutation Strategy for the Novel Family of Quasi-Z-Source AC-AC Converter," IEEE Trans. Ind. Informat., vol.9, no.3, pp.1538–1547, Aug. 2013.

[105] M. Nguyen, Y. Lim, Y. Kim, "A Modified Single-Phase Quasi-Z-Source AC-AC Converter," IEEE Trans. Power Electron., vol.27, no.1, pp.201–210, Jan. 2012.

[106] W. Song, Y. Zhong, H. Zhang, X. Sun, Q. Zhang, W. Wang, "A study of Z-source dual-bridge matrix converter immune to abnormal input voltage disturbance and with high voltage transfer ratio," IEEE Trans. Ind. Informat., vol.9, no.2, pp.828–838, May 2013.

[107] X. Liu, P. C. Loh, P. Wang, X. Han, "Improved modulation schemes for indirect Z-source matrix converter with sinusoidal input and output waveforms," IEEE Trans. Power Electron., vol.27, no.9, pp.4039–4050, Sept. 2012.

[108] B. Ge, Q. Lei, W. Qian, F. Z. Peng, "A family of Z-source matrix converters," IEEE Trans. Ind. Electron., vol.59, no.1, pp.35–46, Jan. 2012.

[109] S. Liu, B. Ge, H. Abu-Rub, F. Z. Peng, and Y. Liu, "Quasi-Z-source matrix converter based induction motor drives," in Proc. 38th Annual Conference on IEEE Industrial Electronics Society (IECON), pp.5303–5307, 2012.

[110] O. Ellabban, H. Abu-Rub, B. Ge, "A Quasi-Z-Source Direct Matrix Converter Feeding a Vector Controlled Induction Motor Drive," IEEE Journal of Emerging and Selected Topics in Power Electronics, vol.3, no.2, pp.339–348, June 2015.

[111] L. Huber, D. Borojevic, "Space vector modulated three-phase to three-phase matrix converter with input power factor correction," IEEE Trans. Ind. Appl., vol.31, no.6, pp.1234–1246, Nov/Dec 1995.

[112] M. Shen, A. Joseph, J. Wang, F. Z. Peng, D. J. Adams, "Comparison of traditional inverters and Z-source inverter for fuel cell vehicles," IEEE Trans. Power Electron., vol.22, no.4, pp.1453–1463, July 2007.

[113] D. Vinnikov, I. Roasto, "Quasi-Z-Source-based isolated DC/DC converters for distributed power generation," IEEE Trans. Ind. Electron., vol.58, pp.192–201, Jan 2011.

[114] I. Roasto, D. Vinnikov, "New voltage mode control method for the quasi-Z-Source-based isolated DC/DC converters," in Proc. 2012 IEEE International Conference on Industrial Technology (ICIT), pp.644–649, 2012.

[115] A. Chub, O. Husev, D. Vinnikov, F. Blaabjerg, "Novel family of quasi-Z-source DC/DC converters derived from current-fed push-pull converters," in Proc. 2014 16th European Conference on Power Electronics and Applications (EPE'14-ECCE Europe), pp.1–10, 2014.

[116] Y. P. Siwakoti, F. Blaabjerg, P. C. Loh, G. E. Town, "High-voltage boost quasi-Z-source isolated DC/DC converter," IET Power Electronics, vol.7, no.9, pp.2387–2395, September 2014.

[117] International contributor for sixth International Edition of "Electrical Engineering (Principles and Applications)" by Allan R. Hambley (ISBN: 978-0-273-79325-0), Pearson Education International , 2013.

[118] International contributor for fourth International Edition of "Power Electronics (Circuits, Devices and Applications)" by Muhammad H. Rashid (ISBN: 978-0-273-769088), Pearson Education International, 2013.

[119] Kurs, A. Karalis, R. Moffatt, J. D. Joannopoulos, P. Fisher, and M. Soljacic, "Wireless power transfer via strongly coupled magnetic resonances,"Science, Vol. 317, pp. 83-86, Jul. 2007.

[120] J. T. Boys and G. A. Covic, "The Inductive Power Transfer Story at the University of Auckland," IEEE Circuits Syst. Mag., Vol. 15, No.2, pp. 6-27, May 2015.

[121] H. Vázquez-Leal, A. Gallardo-Del-Angel, and R. Castañeda- Sheissa, "The Phenomenon of Wireless Energy Transfer: Experiments and Philosophy," in Wireless Power Transfer- Principles and Engineering Explorations, InTech, Chap. 1, pp. 1-18, 2012.

[122] R. Melki and B. Moslem, "Optimizing the design parameters of a wireless power transfer system for maximizing power transfer efficiency: A simulation study," in Technological Advances in Electrical, Electronics and Computer Engineering (TAEECE), pp. 278-282, 2015.

[123] Wang, H. Zhang, and Y. Liu, "Analysis on the efficiency of magnetic resonance coupling wireless charging for electric vehicles," in Cyber Technology in Automation, Control and Intelligent Systems (CYBER), pp. 191-194, 2013.

[124] Kallel, O. Kanoun, T. Keutel, and C. Viehweger, "Improvement of the efficiency of MISO configuration in inductive power transmission in case of coils misalignment," in Instrumentation and Measurement Technology Conference (I2MTC) Proceedings, pp. 856-861, 2014.

[125] M. Fu, T. Zhang, C. Ma, and X. Zhang, "Efficiency and Optimal Loads Analysis for Multiple-Receiver Wireless Power Transfer Systems," IEEE Trans. Microw. Theory Techn., Vol. 63, No. 3, pp. 801-812, Mar. 2015.

[126] Z. Low, R. Chinga, R. Tseng, and J. Lin, "Design and test of a high-power high-efficiency loosely coupled planar wireless power transfer system," IEEE Trans. Ind. Electron., Vol. 56, No. 5, pp. 1801-1812, May 2009.

[127] O. Jonah, S. V. Georgakopoulos, D. Daerhan, and Y. Shun, "Misalignment-insensitive wireless power transfer via strongly coupled magnetic resonance principles," in Antennas and Propagation Society International Symposium (APSURSI), pp. 1343-1344, 2014.

[128] H. Feng, T. Cai, S. Duan, J. Zhao, X. Zhang, and C. Chen, "An LCC-compensated resonant converter optimized for robust reaction to large coupling variation in dynamic wireless power transfer," IEEE Trans. Ind. Electron., Vol. 63, No. 10, pp. 6591-6601, Oct. 2016.

[129] N. Kuyvenhoven, C. Dean, J. Melton, J. Schwannecke, and A. Umenei, "Development of a foreign object detection and analysis method for wireless power systems," in Product Compliance Engineering (PSES) Proceedings, pp. 1-6, 2011.

[130] G. Jang, S. Jeong, H. Kwak, and C. Rim, "Metal object detection circuit with non-overlapped coils for wireless EV chargers," in Southern Power Electronics Conference (SPEC), pp. 1-6, 2016.

[131] L. Tan, S. Pan, C. Xu, C. Yan, H. Liu, and X. Huang, "Study of constant current-constant voltage output wireless charging system based on compound topologies," J. Power Electron., Vol. 17, No. 4, pp. 1109-1116, Jul. 2017.

[132] L. Sun, H. Tang, and C. Yao, "Investigating the frequency for load-independent output voltage in three-coil inductive power transfer system," Int. J. Circ. Theor. Appl, Vol. 44, No. 6, pp. 1341-1348, Aug. 2015.

[133] L. Zhang, X. Yang, W. Chen, and X. Yao, "An isolated soft-switching bidirectional buck-boost inverter for fuel cell applications," J. Power Electron., Vol. 10, No. 3, pp. 235-244, May 2010.

[134] Electrical engineering: principles and applications AR Hambley, N Kumar, AR Kulkarni Pearson Education (New Jersey), 2011.

[135] Power Electronics Devices MH Rashid, N Kumar, A Kulkarni - Circuits and Applications (4th Edition), England, 2014.

LIST OF PUBLICATIONS

[1] Ayush Kumar Srivastava and Narendra Kumar, "Analysis of Z-Source Resonant Converter for Wireless Charging Application", International Conference on RECENT DEVELOPMENTS IN ELECTRICAL AND ELECTRONICS ENGINEERING (ICRDEEE 2022), pp 1-9, J.C. Bose University of Science and Technology, YMCA, Haryana, India, 15-16 April 2022. **(Got Best Paper Award for this conference)**.

[2] Ayush Kumar Srivastava and Narendra Kumar, "Implementation of Z-Source Resonant Converter for Power Factor Correction & Wireless Charging Applications", 2022 Second International Conference on Advances in Electrical, Computing, Communications and Sustainable Technologies (ICAECT 2022), pp 1-6, Shri Shankarachariya Technical Campus (SSTC), Bhilai, Chhattisgarh, India, 21-22 April 2022.